

A Hybrid Genetic Algorithm with Type-Aware Chromosomes for Traveling Salesman Problems with Drone

Sasan Mahmoudinazlou

Department of Industrial and Management Systems Engineering, University of South Florida, Tampa, FL 33620, U.S.A.
sasanm@usf.edu

Changhyun Kwon*

Department of Industrial and Systems Engineering, KAIST, Daejeon, 34141, Republic of Korea
chkwon@kaist.ac.kr
OMELET, Daejeon, 34051, Republic of Korea

Abstract

There are emerging transportation problems known as the Traveling Salesman Problem with Drone (TSPD) and the Flying Sidekick Traveling Salesman Problem (FSTSP) that involve using a drone in conjunction with a truck for package delivery. This study presents a hybrid genetic algorithm for solving TSPD and FSTSP by incorporating local search and dynamic programming. Similar algorithms exist in the literature. Our algorithm, however, considers more sophisticated chromosomes and less computationally complex dynamic programming to enable broader exploration by the genetic algorithm and efficient exploitation through dynamic programming and local search. The key contribution of this paper is the discovery of how decision-making processes for solving TSPD and FSTSP should be divided among the layers of genetic algorithm, dynamic programming, and local search. In particular, our genetic algorithm generates the truck and the drone sequences separately and encodes them in a type-aware chromosome, wherein each customer is assigned to either the truck or the drone. We apply local search to each chromosome, which is decoded by dynamic programming for fitness evaluation. Our new algorithm is shown to outperform existing algorithms on most benchmark instances in both quality and time. Our algorithms found the new best solutions for 538 TSPD instances out of 920 and 74 FSTSP instances out of 132.

Keywords: vehicle routing; traveling salesman problem; genetic algorithm; dynamic programming

1 Introduction

With the growing number of online orders, companies are competing to ship products in a timely manner. This underscores the need for improved delivery methods. Traditional methods include using the Traveling Salesman Problem (TSP), in which a vehicle, perhaps a truck, takes multiple orders and delivers them to customers as soon as possible. As a result of the truck's low speed and need to maneuver around traffic flows, many large companies such as Amazon and UPS are looking for new delivery methods like drones. Unlike traditional trucks, drones do not have to follow the same network, giving them faster delivery times. They are also more eco-friendly since they are electrical and less expensive since they do not require any human involvement.

*Corresponding author

It is important to note that drones also come with some significant limitations. Unlike trucks, drones do not have the capability to carry heavy or multiple parcels. To be able to pick up an item after every delivery, a drone must return to the warehouse. Drones are limited in their range due to their battery capacity and cannot reach remote customers.

Recent efforts have been made to utilize the advantages of both vehicles and include a delivery method in which the truck and the drone collaborate. Murray and Chu (2015) describe the combined problem as the Flying Sidekick Traveling Salesman Problem (FSTSP). The FSTSP extends the traditional Traveling Salesman Problem by introducing a “sidekick” that can fly and assist the salesperson in visiting cities. The challenge is to find the shortest route that allows both the salesperson (ground vehicle) and sidekick (drone) to visit all cities while considering the drone’s limited flying range. The drone lies on top of the truck and can fly at various points, deliver a parcel to a customer, and land on the truck at another point while the truck can make deliveries at the same time. A similar problem is introduced by Agatz et al. (2018) as the Traveling Salesman Problem with Drone (TSPD) with slightly simpler assumptions. The main difference is that the drone can wait for the truck in the TSPD but not in the FSTSP, among other differences in the assumptions. Section 3 provides an in-depth elucidation of the assumptions pertaining to two problems, highlighting their distinct characteristics and points of divergence. We refer readers to Chung et al. (2020) and Macrina et al. (2020) for other problems that involve both ground vehicles and drones.

A hybrid genetic algorithm (HGA) is presented in this study for solving both TSPD and FSTSP with the aim of minimizing total delivery time. While regular genetic algorithms only rely on crossovers and mutations to generate new solutions, hybrid genetic algorithms, also known as memetic algorithms (Moscato et al., 1989), usually improve the generated solutions by local search or other heuristics in addition to those conventional techniques. Hybrid genetic algorithms have been actively developed to solve various vehicle routing problems (Ho et al., 2008; Vidal et al., 2012), including the problem of our interest, TSPD/FSTSP (Ha et al., 2020).

Our HGA approach consists of three layers in its algorithmic structure. First, a regular genetic algorithm (GA) layer generates incomplete solutions by determining the customer nodes served by the truck and the drone, called truck nodes and drone nodes, respectively. Second, a dynamic programming (DP) layer completes the solutions by determining the combined nodes, where the drone departs from the truck or returns to the truck. Third, we use various local search neighborhoods to improve the generated solutions.

The key contribution of this paper is the discovery of how decision-making processes should be divided among these three layers. Similar approaches exist in the literature, especially, Ha et al. (2020), whose GA layer is simple while the difficult decision-making step is handled by their DP layer. We give more informed exploratory roles in the GA layer, while we use a much simpler DP layer so that the decoding and evaluation for exploitation are faster. Our GA layer utilizes a novel type-aware chromosome (TAC) encoding to distinguish truck and drone nodes. We also devise type-aware order crossover operations to support the TAC encoding in the GA layer. Our unique TAC encoding allows the DP layer to have a time complexity of $O(n^2)$, which is lower than other DP-based approaches used in the literature with the time complexities of $O(n^3)$ and $O(n^4)$ (see Section 4.3). With the TAC encoding, it is easy to devise various local search neighborhoods directly on the chromosomes. It is unnecessary to apply additional encoding on the decoded solutions from the DP layer, and it is possible to keep high-resolution information on the solutions in the GA populations. Furthermore, our GA layer uses two or three subpopulations, depending on whether the drone range is limited, and we propose an escaping strategy for preventing GAs from being trapped in local optima. The proposed division of three layers with the TAC encoding brings reduction in the objective function values, savings in the computational time, or both, in most benchmark instances.

The remainder of the paper is organized as follows. A brief summary of the literature is given in Section 2, and a formal definition of the problem is given in Section 3. The methodology is described in Section 4, and the numerical results from the experiments are given in Section 5. Finally, the conclusion and future directions are discussed in Section 6. In the rest of the paper, we call our method the HGA with TAC, or HGA-TAC, to emphasize the significance of the TAC encoding.

2 Literature Review

The number of recent publications that are dedicated to the study of last-mile delivery with truck and drone collaboration is rapidly increasing, and because of this, the majority of the articles that we review are those that are pertinent to our work. We refer to survey papers, Otto et al. (2018), Macrina et al. (2020), Chung et al. (2020), and Li et al. (2021), for general overviews on the optimization of problems with various applications of drones. Several approaches have been taken in the literature to study the collaboration between trucks and drones. Note that the research topics differ regarding the number of vehicles, the basic assumptions and limitations, and the method of solving them. As our study focuses on the collaboration between a single truck and a single drone with only one visit per flight, we review the most relevant papers in this section.

We begin by reviewing the papers that first proposed the problem. Our next step is to review publications that employ heuristic and metaheuristic approaches, followed by those that utilize exact approaches. Lastly, we introduce two papers that use machine-learning techniques to solve the problem.

Murray and Chu (2015) introduce the FSTSP, formulate it using mixed-integer linear programming (MILP), and propose a heuristic algorithm for solving it. To solve the TSPD, Agatz et al. (2018) also propose an MILP formulation, which is computationally tractable for small problems with up to twelve customers. They provide a heuristic algorithm, called ‘TSP-ep-all,’ that combines neighborhood search and a partitioning algorithm, which begins with an optimal or near-optimal TSP tour. Given the initial TSP tour, they use a DP approach to determine which customers should be visited by the drone, while maintaining the order in the given TSP tour. This procedure is called the *exact partitioning* of customers. Then, the TSP-ep-all algorithm generates other TSP tours by perturbing the TSP tour using local search neighborhoods such as the two-opt swap, the three-opt swap, and the two-point swap, which are popularly used in TSP heuristics. For each generated TSP tour, the exact partitioning is used to create a TSPD solution. The algorithm returns the minimal delivery time TSPD solution as the final solution. This method has been shown to be efficient and effective in small to medium-sized problems with less than 50 customers, but it shows exponentially increasing computational time due to the extensive local search on the initial TSP tour. They also created a benchmark TSPD dataset, which we will use to compare our algorithm with other methods.

A Divide-Partition-and-Search heuristic (DPS) was introduced by Boggyrbayeva et al. (2023) for solving TSPD. In the DPS approach, the network is systematically divided into smaller problems, drawing inspiration from the divide-and-conquer heuristic proposed by Poikonen et al. (2019). Each resulting subproblem is then addressed using the TSP-ep-all algorithm (Agatz et al., 2018). Specifically, DPS/ g partitions all nodes into subgroups, each containing g nodes. Subsequently, each subgroup undergoes a partitioning process facilitated by TSP-ep-all. It is noteworthy that when g equals the total number of nodes (N), DPS/ N is equivalent to TSP-ep-all. The performance of DPS exhibits improvement with an increase in g , albeit at the expense of longer solution times. However, DPS/25 demonstrates commendable performance, proving to be notably faster than TSP-ep-all, especially for larger instances. Consequently, DPS/25 is selected as a primary baseline algorithm for comparative analysis in this study.

Various metaheuristic methods have been developed successfully for solving TSPD/FSTSP in the

literature. Most related to our approach is the Hybrid General Variable Neighborhood Search (HGVNS) of de Freitas and Penna (2020) and the Hybrid Genetic Algorithm (HGA20) of Ha et al. (2020); not to be confused with our HGA approach, we use the acronym ‘HGA20’ for the method of Ha et al. (2020) throughout the paper. HGVNS also starts with an optimal or near-optimal TSP solution and then converts it to an initial solution by creating sub-routes for the drone. Finally, HGVNS improves the solution by a variable neighborhood search. HGA20 represents each chromosome in the form of a giant tour that corresponds to the TSP tour with the depot removed. The SPLIT method, a polynomial time algorithm proposed in Ha et al. (2018), is employed at each step in order to convert the giant tour chromosome into the FSTSP tour. Then, local search neighborhoods are applied for improvement, and finally, using a restore method, the improved FSTSP tour is converted back into the giant tour chromosome. The chromosome encoding in our approach, however, includes the truck sequence as well as the drone sequence. Only the locations of drone launches and landings remain undecided, which are determined by DP in an optimal manner.

Other metaheuristic methods for TSPD/FSTSP include a greedy randomized adaptive search procedure (Ha et al., 2018), a multi-start variable neighborhood search (Campuzano et al., 2021), and a multi-start tabu search (Luo et al., 2021).

Numerous studies have attempted to solve TSPD using exact methods. A DP approach is developed by Bouman et al. (2018) in order to find an optimal solution to TSPD. Their DP algorithm is able to solve the problem with up to 20 customers. The branch-and-bound algorithm proposed by Poikonen et al. (2019) is also capable of solving TSPD up to 20 nodes at optimum. Additionally, they devise a divide-and-conquer heuristic based on their branch-and-bound algorithm that delivers high-quality solutions. Boccia et al. (2021) introduce a new representation of the FSTSP based on the definition of an extended graph. They present a new MILP formulation and a branch-and-cut algorithm for solving the problem, which is able to find optimal solutions for problems with up to 20 customers. Roberti and Ruthmair (2021) create a new MILP formulation that is more effective and able to accommodate a variety of side constraints. They propose a branch-and-price approach wherein they establish a set partitioning problem and then use the *ng*-route relaxation (Baldacci et al., 2011) to formulate the pricing problem. Their technique optimally solves TSPD instances for problems with up to 39 customers. Yang et al. (2023) propose a branch-and-price algorithm for solving the TSPD under uncertainty. The problem is referred to as the robust drone-truck delivery problem (RDTDP). They are able to solve instances of up to 40 customers using their algorithm.

The use of learning-based methods has been reported in a few papers that address TSPD. The K-Means Clustering algorithm is employed by Ferrandez et al. (2016) to determine launch locations, and a GA is used to solve a TSP and determine the truck routes. As part of their objective function, they also aim to minimize the amount of energy consumed as well as the delivery time. The study also examines the case of multiple drones per truck. Bogyrbayeva et al. (2023) design and train a deep reinforcement learning algorithm for solving TSPD and examine it on instances with up to 100 nodes in size. Aside from the training time, their algorithm is capable of solving instances within a relatively short period of time.

Most studies have focused either on TSPD or FSTSP, with a few exceptions, such as de Freitas and Penna (2020), which solves the problem in both settings. It is also important to note that the existing algorithms for TSPD are not exempt from the trade-off rule between solution quality and running time. This work aims to solve both problems, with a particular focus on the disparities in underlying assumptions, and testing on a range of instances from the literature reveals that our method can provide viable solutions in a reasonable amount of time.

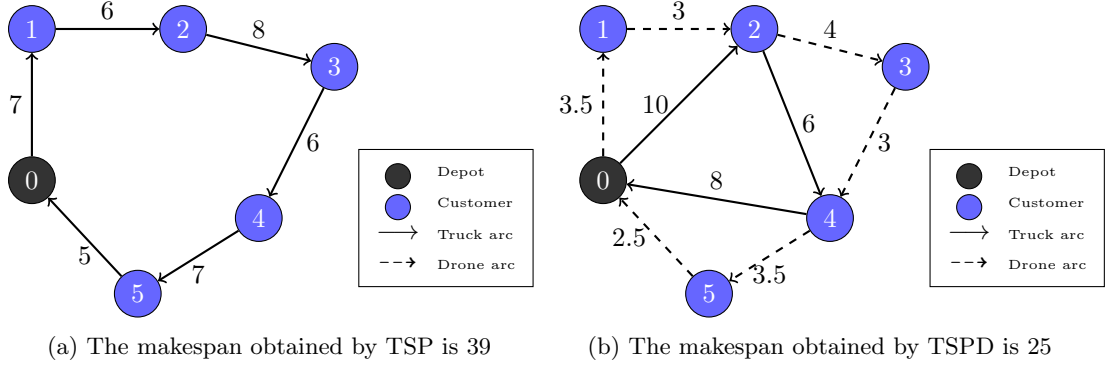


Figure 1: A network with one depot and 5 customers solved by TSP and TSPD.

3 Problem Statement

In this section, we introduce TSPD and FSTSP formally and describe their associated assumptions. As explained before, the TSPD/FSTSP system involves coordinating a truck with a drone to deliver goods with the objective of minimizing the total delivery time, also known as the *makespan* in the operations research literature. For the rest of the paper, we will use the term *makespan* as our objective function. As the drone resides on the truck's roof, it can be launched to deliver a package to a customer and then return to the top of the truck. The TSPD can be represented on a graph $G(\mathcal{V}, \mathcal{E})$ where $\mathcal{V} = \{0, 1, \dots, n\}$ is the set of nodes, n is the number of customer nodes, and \mathcal{E} is the set of edges of the graph which is assumed to be complete. We let $N = |\mathcal{V}| = n + 1$. Vehicles start their routes at the depot node 0 and must return to it after completing their deliveries; for returning, the depot is represented as $0'$. The remaining nodes refer to the locations of customers. The travel time between the nodes may vary in accordance with the type of vehicle and the assumptions made about the problem. The ratio of drone speed to truck speed is represented by α . For instance, if $\alpha = 2$ and the Euclidean distance is used for both vehicles, the travel time for a drone between two geographical locations will be half of the time required for a truck to travel between the same nodes.

Before delving into the specifics, let us consider an illustrative example of a simple network solved using TSPD and the amount of time saved over regular TSP. Figure 1a depicts the optimal TSP solution for a network with one depot and five customers, whereas Figure 1b illustrates the same network utilizing a truck and a drone in collaboration. Numbers on the arcs indicate traversal times for corresponding vehicles with $\alpha = 2$. The set of deliveries made by the cooperation of two vehicles between each launch and land is named an *operation* by Agatz et al. (2018) and *sortie* by Murray and Chu (2015). Each operation is defined as $\langle i, j, k \rangle$, where i is the position where the drone launches, j is the location where the customer is served, and k is the position where the drone lands on the truck. In the first operation $\langle 0, 1, 2 \rangle$, for instance, the drone takes off from the depot, makes a delivery to the customer at node 1, and lands on the truck at node 2. The minimum time for each operation can be calculated as $\max\{\tau_{i \rightarrow k}^{\text{tr}}, \tau_{i,j}^{\text{dr}} + \tau_{j,k}^{\text{dr}}\}$ where $\tau_{i \rightarrow k}^{\text{tr}}$ is truck's travel time from i to k traversing all the nodes in between if any, and $\tau_{i,j}^{\text{dr}}$ is drone's travel time between two nodes. In this simplified instance, TSPD shows a 36 percent improvement over TSP, which indicates that drones can serve a valuable and beneficial function for last-mile delivery.

We first state the common assumptions of the TSPD and FSTSP, and then problem-specific assumptions.

3.1 Common Assumptions

Both TSPD and FSTSP make the following assumptions:

1. Both vehicles start their tour at the depot and must return there at the end of their tour after completing all deliveries.
2. In each operation, the drone is only permitted to visit one customer before returning to either the truck or depot. While the drone is in flight, the truck can make multiple deliveries.
3. Drone launches only at customer locations or depot 0 and lands only at customer locations or depot 0'.
4. Each customer is visited only once by either the drone or the truck. While customers are served by the truck, the drone might be onboard with the truck or in flight.

3.2 Problem-Specific Assumptions

All of the above general assumptions hold true for both TSPD and FSTSP, whereas the specific assumptions for each problem are listed below.

1. *Launch and landing nodes*: In both cases, the drone can be relaunched from the same spot on the vehicle where it landed. However, in FSTSP, drones cannot land on the same node from where they are launched, but in TSPD, this is permitted.
2. *Setup times*: TSPD disregards pickup time, delivery time, and recharging (battery changing) time, whereas FSTSP includes preparation time denoted s_L before a launch for changing the battery and loading the cargo, and retrieval time when landing on the truck denoted s_R .
3. *Drone eligible nodes*: In TSPD, all customers can be visited and serviced by either vehicle; however, in FSTSP, some customers cannot be visited by drone for a variety of reasons. It could be due to a heavy package that cannot be carried by a drone, the necessity for a signature, or an impractical landing site.
4. *Flying range*: The drone has a limited flight time due to its limited battery capacity. Agatz et al. (2018) solves the problem with the assumption of limited and unlimited flying range for the drone. In TSPD, the flying range constraint just contains the time that a drone flies between nodes, whereas in FSTSP, it also includes the time that the drone must remain in constant flight if waiting for the truck at the rendezvous point, as it is not permitted to land and wait for the truck. For this reason, each FSTSP operation must satisfy the drone's flying endurance constraint for the truck as well. For clarity, let e represent the drone's endurance. For operation $\langle i, j, k \rangle$, the relevant TSPD constraint for the drone solely is:

$$\tau_{i,j}^{\text{dr}} + \tau_{j,k}^{\text{dr}} \leq e.$$

While in the case of FSTSP, the constraint is:

$$\max\{\tau_{i,j}^{\text{dr}} + \tau_{j,k}^{\text{dr}} + s_R, \tau_{i \rightarrow k}^{\text{tr}} + s_T\} \leq e.$$

where $\tau_{i \rightarrow k}^{\text{tr}}$ denotes the time required for the truck to travel from node i to k while fulfilling deliveries en route, and s_T represents the time needed for the truck to recover the drone and potentially prepare it for subsequent launches. In precise terms, when the drone is solely recovered without relaunching at the same location, the service time s_T is equivalent to the recovery time s_R . Conversely, if the truck chooses to relaunch the drone at the same location, the preparation time for the drone's subsequent launch (s_L) is added to the service time, resulting in $s_T = s_R + s_L$. There is no such constraint when the launch node is the depot.

Despite the fact that these problem names have been used interchangeably in the literature, or some studies may include a combination of these assumptions, we tried to categorize the assumptions based on the first two papers that introduce the problem. In this study, we address both of these problems in our algorithm, solve instances from both natures, and compare our results with the best current methods. These differences in the problem assumptions are handled mainly in the DP layer.

4 A Hybrid Genetic Algorithm with Type-Aware Chromosomes

In this section, we describe the structure of our GA, provide the local search neighborhoods, expound our DP technique, and introduce our strategy for escaping local optima.

The algorithm we propose is a HGA similar to Vidal et al. (2012) in terms of its basic construction. We search for both feasible and infeasible solutions stored in two or three subpopulations. Additionally, we take advantage of the contribution each individual provides to the diversity of the gene pool rather than only considering the cost of the solution. Ha et al. (2020) also employ this structure for solving FSTSP but use a completely different representation of solutions and fitness evaluation technique from ours, as it will be explained in Section 4.3.

Algorithm 1 displays our HGA’s general structure. The algorithm commences by initializing the subpopulations, as elucidated in Section 4.2 (Lines 1-4). The feasible, Type 1 infeasible, and Type 2 infeasible subpopulations are denoted by Ω_F , Ω_{INF}^1 , and Ω_{INF}^2 . Individuals with the characteristic of more than one node being visited by the drone in a single flight are placed into the Type 1 infeasible subpopulation. Solutions exceeding the drone’s range limit are classified into the Type 2 infeasible subpopulation. It should be noted that if the range of the drone is unlimited, the use of Ω_{INF}^2 will be irrelevant, and we would only consider Ω_F and Ω_{INF}^1 .

Once the initial population is generated, the iterative process continues until a convergence criterion is met, where convergence is defined as no observed improvement for a predefined number of iterations, denoted as It_{NI} . At each iteration, two parents are selected from the entire population (Line 6), subjected to a crossover operation (Line 7), resulting in the generation of a new offspring. This offspring, with a probability P_M , undergoes a mutation operation (Line 8). Explicit details regarding parent selection, crossover, and mutation are expounded upon in Section 4.4.

After generation, the offspring undergoes an evaluation to determine its feasibility and corresponding fitness (Line 9). If the offspring is deemed infeasible, the fitness incorporates penalties. The evaluation process intricacies are outlined in Section 4.3. In the event of infeasibility, the algorithm makes the solution feasible with probability P_{REPAIR} (Lines 14, 15). The repair procedure is straightforward: when a violation occurs with respect to any of the drone constraints, the associated node changed to be a truck node. Specifically, if the solution entails consecutive drone nodes within a single flight or includes flights that violate the drone range constraint, the node types are adjusted to be serviced by trucks instead. The offspring is subsequently incorporated into the feasible or infeasible subpopulation based on its feasibility status. Should the offspring exhibit feasibility, local search neighborhoods are applied to enhance solution quality (Lines 10 and 16), with detailed explanations of local search neighborhoods provided in Section 4.5.

If any of the subpopulations attain a size of $\mu + \lambda$, the algorithm selectively retains the best μ solutions while discarding the remainder (Lines 26-30). Concurrently, the algorithm dynamically manages the generation of infeasible solutions by iteratively adjusting infeasibility penalties (Line 31) (Section 4.6 provides comprehensive details). In instances where the solution fails to exhibit improvement after It_{DIV} iterations, a population diversification strategy is employed (Lines 32-34). In this step, the first n_{BEST} individuals are retained and the rest will be removed. Then new individuals will be generated

Algorithm 1 Hybrid Genetic Algorithm with Type-Aware Chromosomes

```

1:  $\Omega_F \leftarrow \emptyset$  ▷ Feasible subpopulation
2:  $\Omega_{INF}^1 \leftarrow \emptyset$  ▷ Infeasible subpopulation (Type 1)
3:  $\Omega_{INF}^2 \leftarrow \emptyset$  ▷ Infeasible subpopulation (Type 2)
4:  $\Omega_F, \Omega_{INF}^1, \Omega_{INF}^2 = \text{initial\_population}()$  ▷ Algorithm 2
5: while number of iterations with no improvement  $< It_{NI}$  do
6:   Select  $\omega_1$  and  $\omega_2$  from  $\Omega_F \cup \Omega_{INF}^1 \cup \Omega_{INF}^2$ 
7:    $\omega \leftarrow \text{crossover}(\omega_1, \omega_2)$ 
8:    $\text{mutate}(\omega)$ 
9:   if  $\omega$  is feasible then
10:      $\text{local\_search}(\omega)$ 
11:      $\Omega_F \leftarrow \Omega_F \cup \{\omega\}$ 
12:   else
13:      $r \leftarrow \text{rand}(0, 1)$ 
14:     if  $r < P_{\text{REPAIR}}$  then
15:       Make  $\omega$  feasible
16:        $\text{local\_search}(\omega)$ 
17:        $\Omega_F \leftarrow \Omega_F \cup \{\omega\}$ 
18:     else
19:       if  $\omega$ 's infeasibility is Type 1 then
20:          $\Omega_{INF}^1 \leftarrow \Omega_{INF}^1 \cup \{\omega\}$ 
21:       else
22:          $\Omega_{INF}^2 \leftarrow \Omega_{INF}^2 \cup \{\omega\}$ 
23:       end if
24:     end if
25:   end if
26:   for  $\Omega \in \{\Omega_F, \Omega_{INF}^1, \Omega_{INF}^2\}$  do
27:     if  $\text{size}(\Omega) = \mu + \lambda$  then
28:        $\text{select\_survivors}(\Omega)$ 
29:     end if
30:   end for
31:   Adjust penalties
32:   if  $\text{best}(\Omega_F)$  not improved for  $It_{DIV}$  iterations then
33:      $\text{diversify}(\Omega_F, \Omega_{INF}^1, \Omega_{INF}^2)$ 
34:   end if
35:   if  $\text{best}(\Omega_F)$  not improved for  $It_{LOC}$  iterations then
36:      $\text{escape\_local\_optima}(\text{best}(\Omega_F))$ . ▷ Algorithm 4
37:   end if
38: end while
39: Return  $\text{best}(\Omega_F)$ 

```

according to Algorithm 2 until each subpopulation size reaches μ (Section 4.6). Additionally, if no enhancements are observed after It_{LOC} iterations, the algorithm endeavors to escape from local optima using an alternative technique expounded upon in Section 4.7 (Lines 35-37). It is pertinent to emphasize that $It_{\text{DIV}} < It_{\text{LOC}} < It_{\text{NI}}$.

4.1 Type-Aware Chromosome Encoding

The route taken by each vehicle, as well as the locations where the drone is launched from and lands on the truck, are the solutions to the TSPD and the FSTSP. Our HGA for TSPD/FSTSP is unique in how we encode each solution in a chromosome, which keeps a sequence of customer nodes and records the type of each node: either a truck node or a drone node. Hence, we call our HGA the HGA with Type-Aware Chromosomes (HGA-TAC). While each number in HGA-TAC’s Chromosome encoding represents a customer node in the sequence, the truck nodes are represented by positive numbers, and the drone nodes are shown by negative numbers. Therefore, each chromosome includes the truck route as well as the drone route, and the TSPD/FSTSP tour will be accomplished if the launch and landing points are known. To handle such type-aware chromosomes, we devise a novel DP formulation and type-aware crossover operations. The proposed DP method, which we call JOIN, determines the optimal launch and landing points for the drone. The details of the JOIN algorithm are discussed in Section 4.3.

A simple example will serve as a better understanding of our chromosome encoding. Consider a network that has ten customers. Figure 2a illustrates how the chromosome of an individual is coded in our algorithm before and after the addition of the depot. As mentioned previously, positive and negative numbers represent the nodes visited by truck and drone, respectively. The truck tour in this example is $[0, 4, 6, 9, 3, 1, 10, 0']$, while the drone tour is $[0, 2, 5, 8, 7, 0']$. The TSPD solution is shown in Figure 2b if we assume the launch and landing locations found by JOIN are $\{0, 6, 3, 10\}$ and $\{6, 3, 1, 0'\}$ respectively.

4.2 Generating Initial Subpopulations

In the case, like ours, that the drone is limited to only one customer per flight, any two or more consecutive negative numbers would be considered infeasible (Type 1) in our chromosome encoding. Additionally, if the drone’s flight range is restricted, a representation can be evaluated for feasibility (Type 2). Therefore, when the drone range is unlimited, our GA will consist of two subpopulations; otherwise, it will consist of three subpopulations.

Algorithm 2 illustrates how the initial population is generated. Initially, we find a TSP solution, then promote it to a TSPD solution using the exact partitioning proposed in Agatz et al. (2018). The initial TSP solution is found using the LKH library (Helsgaun, 2000), an efficient and improved implementation of the Lin-Kernighan algorithm (Lin and Kernighan, 1973). To diversify the population and explore the solution space effectively, new individuals are generated by applying specific modifying operators to existing solutions. The process involves the utilization of two distinct operators, each contributing to the exploration of different aspects of the search space.

Element-Wise Modification: This operator involves the random modification of individual elements within a chromosome. Specifically, for each element in the chromosome, one of the following actions is randomly chosen: sign change, element swap with the successor, or no action. The selection of actions is governed by random numbers in the range $[0, 1]$. If the randomly generated number falls within the range $[0, 0.1]$, a sign change is applied to the element. In the range $(0.1, 0.2]$, a swap with the succeeding element takes place. For numbers beyond 0.2, no action is executed, leaving the element unaltered (Lines 8-11).

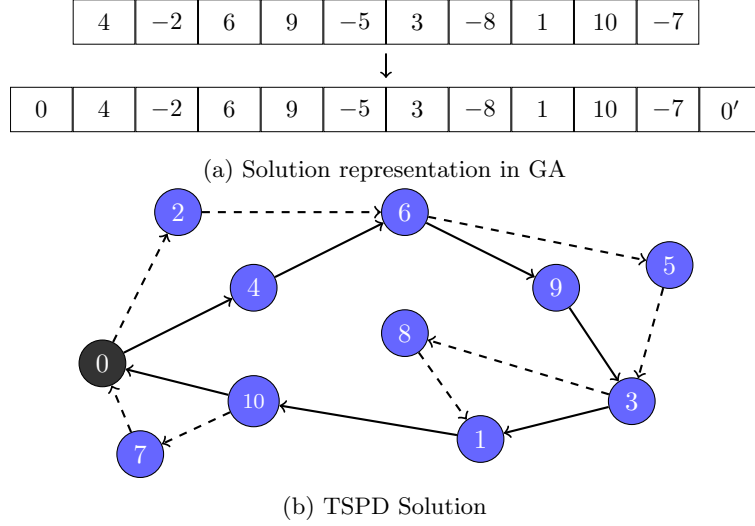


Figure 2: For a network of one depot and 10 customers, the figure in (a) is the solution representation, and (b) is the same solution shown on network.

Sequence Modification: This operator introduces variability by modifying subsequences within the chromosome. Two indices, i and j , are randomly selected, and one of the following operations is performed on the sequence between i and j (inclusive): reverse sequence, sign change within the sequence, or shuffle sequence. The choice of operation is determined randomly (Lines 13,14).

It is imperative to iterate through the aforementioned process until each subpopulation attains a population size of μ .

4.3 Decoding and Evaluating Chromosomes by Dynamic Programming

The objective of this section is to propose a DP approach, JOIN, to determine the best launch and landing points according to the sequence and type of vehicles used at each node. Initially, we will formulate the JOIN algorithm to address sequences that adhere to feasibility constraints. Subsequently, we will elucidate the necessary modifications required to extend the algorithm's capabilities in handling various types of infeasible sequences.

As a sub-problem, let us refer to $C(i)$ as the shortest time from truck node i to the return depot. By formulating an efficient DP formulation that reduces the entire problem to these subproblems, the optimal objective can be achieved. The minimum makespan will be represented by $C(0)$. Following is a list of the notation, state transitions, and optimal decisions for a given chromosome being evaluated by JOIN:

- $\tau_{i \rightarrow k}^{\text{tr}}$: Truck travel time from node i up to node k (visiting all the nodes in between).
- $\tau_{i,j}^{\text{dr}}$: Drone travel time from node i to node j .
- i : The current truck node in the sub-problem.
- $C(i)$: Shortest time of the system of truck and drone from node i to the depot $0'$.
- $d(i)$: The closest drone node superseding node i in the chromosome representation (If none, then it would be a dummy node after the depot.)
- $d^+(i)$: The drone node superseding $d(i)$ in the chromosome representation (If none, then it would be a dummy node.)

Algorithm 2 Initial Population

```

1: TSP_tour  $\leftarrow$  LKH(Network)
2:  $\omega_0 \leftarrow$  PARTITION(TSP_tour)  $\triangleright$  Exact Partitioning by Agatz et al. (2018)
3:  $\Omega_F \leftarrow \{\omega_0\}, \Omega_{INF}^1 \leftarrow \emptyset, \Omega_{INF}^2 \leftarrow \emptyset$   $\triangleright$  Feasible and infeasible subpopulations
4: while Size of any subpopulation  $< \mu$  do
5:    $\omega \leftarrow \omega_0$ 
6:    $r \leftarrow \text{rand}(0, 1)$ 
7:   if  $r < 0.5$  then
8:     for each  $i \in 1 : n$  do
9:       With probability 0.1:  $\omega[i] \leftarrow -\omega[i]$ 
10:      With probability 0.1: swap( $\omega[i], \omega[i+1]$ ) or swap( $\omega[i], \omega[i-1]$ )
11:    end for
12:  else
13:    Randomly choose  $i_1$  and  $i_2$  from  $1, 2, \dots, n$ 
14:     $\omega[i_1 : i_2] \leftarrow \omega[i_2 : i_1]$  or  $-\omega[i_1 : i_2]$  or shuffle( $\omega[i_1 : i_2]$ )
15:  end if
16:  if  $\omega$  is feasible then
17:     $\Omega_F \leftarrow \Omega_F \cup \{\omega\}$ 
18:  else
19:    if  $\omega$  is Type 1 infeasible then
20:       $\Omega_{INF}^1 \leftarrow \Omega_{INF}^1 \cup \{\omega\}$ 
21:    else
22:       $\Omega_{INF}^2 \leftarrow \Omega_{INF}^2 \cup \{\omega\}$ 
23:    end if
24:  end if
25: end while

```

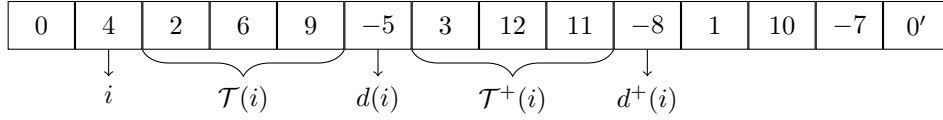


Figure 3: An instance illustrating the notation used in the DP approach

- $\mathcal{T}(i)$: The set of truck nodes between i and $d(i)$.
- $\mathcal{T}^+(i)$: The set of truck nodes between $d(i)$ and $d^+(i)$.

For the reader's convenience, Figure 3 illustrates an example of the representation along with DP notation.

In each state i , the goal is to determine the best move based on the previously computed values and select one of two options, either moving the truck from i to a node in $\mathcal{T}(i)$ while the drone is onboard, or launching the drone from i to visit $d(i)$ and land on a node in $\mathcal{T}^+(i)$ while the truck is visiting all the nodes in between. For TSPD, the last node of $\mathcal{T}(i)$ must be added to $\mathcal{T}^+(i)$, since the drone is permitted to launch, visit a node, and land, while the truck remains stationary. Let us refer to the first type of decision as MT (move the truck) and the second type as LL (launch and land).

The transition of states happens as follows:

1. Let $C_{MT}(i)$ represent the shortest time from node i where the initial decision is to move the truck from i while the drone is onboard. Thus, the required recursion is:

$$C_{MT}(i) = \begin{cases} \infty & \text{if } \mathcal{T}(i) = \emptyset, \\ \min_{k \in \mathcal{T}(i)} \{ \tau_{i \rightarrow k}^{\text{tr}} + C(k) \} & \text{otherwise.} \end{cases}$$

2. In the same manner, let $C_{LL}(i)$ be the shortest possible time from node i , where the first decision is to send the drone from i to serve $d(i)$ and then to land on the truck at some node in $\mathcal{T}^+(i)$. Based on the different assumptions in TSPD and FSTSP, we must have different functions to calculate $C_{LL}(i)$. For TSPD, let $\mathcal{E}^+(i) = \{k \in \mathcal{T}^+(i) : \tau_{i,d(i)}^{\text{dr}} + \tau_{d(i),k}^{\text{dr}} \leq e\}$, which is a subset of $\mathcal{T}^+(i)$ and every node in it can form a feasible drone operation with i and $d(i)$. Therefore, the required recursion for TSPD will be:

$$C_{LL}(i) = \begin{cases} \infty & \text{if } \mathcal{E}^+(i) = \emptyset, \\ \min_{k \in \mathcal{E}^+(i)} \left\{ \max \{ \tau_{i \rightarrow k}^{\text{tr}}, \tau_{i,d(i)}^{\text{dr}} + \tau_{d(i),k}^{\text{dr}} \} + C(k) \right\} & \text{otherwise.} \end{cases}$$

For FSTSP, on the other hand, we need to know whether a drone launch has occurred in node k . Therefore, let σ_k be:

$$\sigma_k = \begin{cases} 1 & \text{if the drone is launched at node } k \\ 0 & \text{otherwise.} \end{cases}$$

Now we define $\mathcal{E}^+(i) = \{k \in \mathcal{T}^+(i) : \tau_{i \rightarrow k}^{\text{tr}} + s_R + \sigma_k s_L \leq e, \tau_{i,d(i)}^{\text{dr}} + \tau_{d(i),k}^{\text{dr}} + s_R \leq e\}$. Therefore, the required recursion for FSTSP will be:

$$C_{LL}(i) = \begin{cases} \infty & \text{if } \mathcal{E}^+(i) = \emptyset, \\ \min_{k \in \mathcal{E}^+(i)} \left\{ \max \{ \tau_{i \rightarrow k}^{\text{tr}} + s_R + \sigma_k s_L, \tau_{i,d(i)}^{\text{dr}} + \tau_{d(i),k}^{\text{dr}} + s_R \} + C(k) \right\} & \text{otherwise.} \end{cases}$$

3. Finally the required recursion for state transition is:

$$C(i) = \min \{ C_{MT}(i), C_{LL}(i) \},$$

where $C(0') = 0$. Therefore, the JOIN algorithm finds the rendezvous points as well as the minimum total time through backward recursion. Note that $\mathcal{E}^+(i) = \emptyset$ and $\mathcal{T}(i) = \emptyset$ would never happen simultaneously. Therefore, $C(i)$ will always have a finite value for any state i .

Following the detailed explanation of the algorithm, we present a formal summary of the JOIN algorithm tailored for feasible TSPD sequences in Algorithm 3. The algorithm ensures optimality through a process of backward propagation, wherein, at each stage, it systematically identifies the minimum makespan from node i to the return depot node by examining all feasible movements. Additionally, it is noteworthy that Algorithm 3 can be readily adapted to accommodate feasible FSTSP sequences by substituting the equation for $C_{LL}(i)$. Subsequent instructions on the necessary modifications to enable JOIN to handle infeasible sequences will be provided shortly.

The time complexity analysis of the algorithm reveals an efficient computational structure. The initial loop traverses all truck nodes, denoted by m , where $m \leq n$. Within this primary loop, two nested loops are implemented. The first inner loop iterates over $k \in \mathcal{T}(i)$, where $|\mathcal{T}(i)| < m$. Simultaneously, the second inner loop iterates over $k \in \mathcal{E}^+(i)$, where $|\mathcal{E}^+(i)| \leq |\mathcal{T}^+(i)| < m$. As a result of this structured arrangement, the worst-case time complexity of the algorithm is $O(n^2)$. This complexity arises from the combination of traversing all truck nodes, the limited cardinality of the sets $\mathcal{T}(i)$ and $\mathcal{E}^+(i)$, ensuring an efficient and scalable computational performance even in larger problem instances.

Lemma 1. *By using the JOIN algorithm for a given chromosome where the sequence and types of the vehicles are known, TSPD (or FSTSP) solutions can be determined in time $O(n^2)$.*

Algorithm 3 JOIN algorithm for finding optimal launch and land locations.

```

1: Set of all truck nodes:  $\{0, i_1, i_2, \dots, i_m, 0'\}$  ( $m \leq n$ )
2:  $C(i) = \infty, C_{MT}(i) = \infty, C_{LL}(i) = \infty$  for  $i = 0, i_1, i_2, \dots, i_m$  ▷ Initialization
3:  $C(0') = 0$ 
4: for  $i = i_m, i_{m-1}, \dots, i_1, 0$  do
5:   for  $k \in \mathcal{T}(i)$  do
6:     if  $\tau_{i \rightarrow k}^{tr} + C(k) < C_{MT}(i)$  then
7:        $C_{MT}(i) = \tau_{i \rightarrow k}^{tr} + C(k)$ 
8:     end if
9:   end for
10:  for  $k \in \mathcal{E}^+(i)$  do
11:    if  $\max\{\tau_{i \rightarrow k}^{tr}, \tau_{i, d(i)}^{dr} + \tau_{d(i), k}^{dr}\} + C(k) < C_{LL}(i)$  then
12:       $C_{LL}(i) = \max\{\tau_{i \rightarrow k}^{tr}, \tau_{i, d(i)}^{dr} + \tau_{d(i), k}^{dr}\} + C(k)$ 
13:    end if
14:  end for
15:   $C(i) = \min\{C_{MT}(i), C_{LL}(i)\}$ 
16: end for
17: return  $C(0)$ 

```

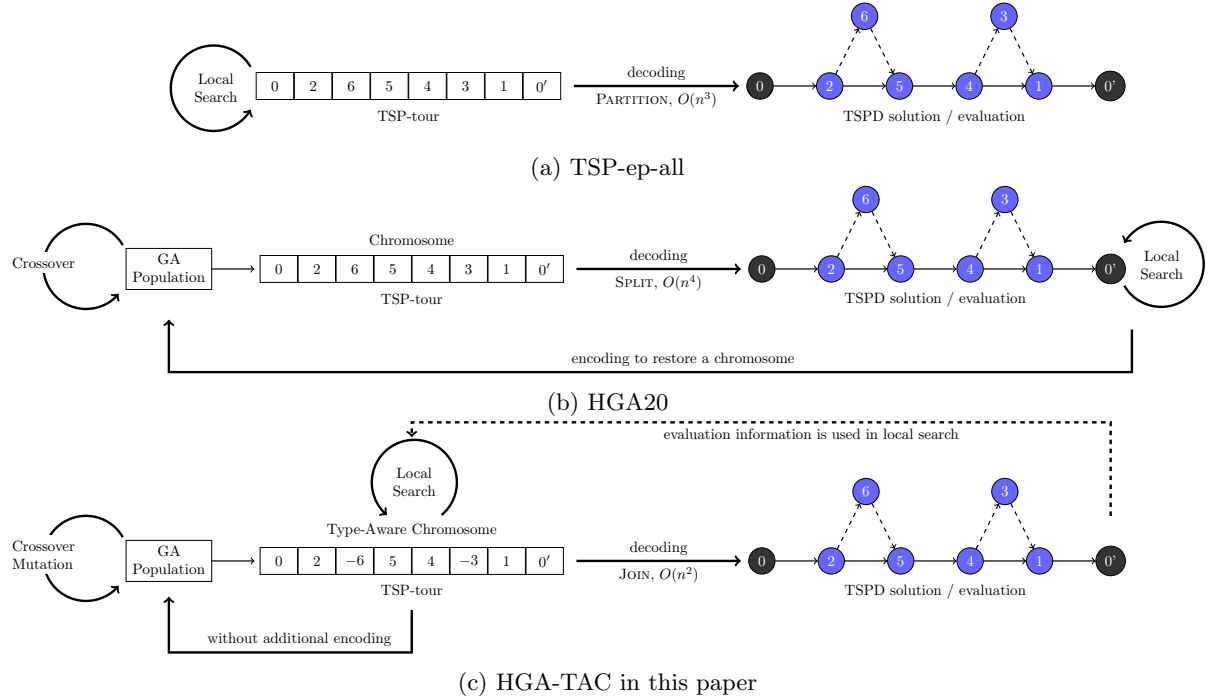


Figure 4: Comparing the structure of our approach to TSP-ep-all in Agatz et al. (2018) and HGA20 in Ha et al. (2020)

With the aim of demonstrating the importance of JOIN’s low time complexity, we now seek to conduct a comparative examination of our algorithm’s structure in relation to TSP-ep-all and HGA20. To facilitate this comparison, Figure 4 presents a comprehensive depiction of our algorithm’s architecture, allowing for a thorough analysis and contrasting of its attributes with those of TSP-ep-all and HGA20. Observably, TSP-ep-all takes a TSP tour and applies exact partitioning, or PARTITION, to transform it optimally to a TSPD solution with time complexity of $O(n^3)$ (Agatz et al., 2018), n being the number of customer nodes. In HGA20, multiple TSP tours are generated by crossover within GA, and the TSPD solution is obtained using the SPLIT method with a time complexity of $O(n^4)$ (Ha et al., 2018), which is analogous to PARTITION. Then the TSPD solution is restored as a chromosome (TSP tour) and reintroduced to the GA population pool.

In our methodology, each chromosome is designed to store more information. GA also determines the vehicle type used to serve each customer, in addition to the order. As illustrated in Figure 4c, each chromosome consists of a sequence of numbers that represent the customers. The positive and negative numbers indicate the customers that will be visited by truck and drone, respectively. To achieve the TSPD solution, it is sufficient to establish where the drone is released from and returns to the truck. The JOIN algorithm is employed to discover the optimal rendezvous points, with the time complexity of $O(n^2)$. To summarize, the type of vehicle required for each node is decided in PARTITION and SPLIT, in addition to rendezvous points, while in our JOIN approach, the first decision has been assigned to GA.

There is another point of comparison that can be drawn between these three approaches: local search. The TSP-ep-all algorithm executes local search on TSP tours before applying PARTITION, while the HGA20 algorithm performs local search after applying SPLIT on TSPD solutions before converting back to chromosomes. Our approach integrates these techniques directly onto the chromosome. Unlike HGA20, which necessitates a conversion back to the chromosome after local search, our method streamlines the process by conducting the local search directly on the chromosome. This modification eliminates the need for an additional encoding step.

Evaluation of infeasible sequences

It is essential to emphasize that the JOIN procedure presented in Algorithm 3 is intended to compute the shortest possible time for feasible solutions. Given that infeasible solutions are ultimately unfavorable, they must be penalized during the evaluation process. The JOIN algorithm will be able to calculate the makespan for infeasible solutions with some slight modifications, denoted as penalized makespan. As previously stated, we exploit two types of infeasibility. For representations with at least two adjacent negative nodes, the drone violates the premise of a single visit per fly. Let $w_1 > 1$ be the penalty for this type of infeasibility (Type 1). The travel time for drone launching at i , visiting j_1, j_2, \dots, j_l and landing at k , will be calculated as $\tau_{i,j_1}^{\text{dr}} + \sum_{q=1}^{l-1} w_1^q \tau_{j_q,j_{q+1}}^{\text{dr}} + \tau_{j_l,k}^{\text{dr}}$.

On the other hand, if the flying range is violated by the drone in TSPD or by any of the vehicles in FSTSP, the solution is Type 2 infeasible. With only a few modifications, the same recursions can be used to calculate the cost. To begin with, set $\mathcal{E}^+(i)$ should be replaced with set $\mathcal{T}^+(i)$, since all movements are possible, regardless of whether or not the drone range constraint is violated. Let w_2 be the penalty for Type 2 infeasibility. For TSPD we only need to add $w_2 \max\{0, \tau_{i,d(i)}^{\text{dr}} + \tau_{d(i),k}^{\text{dr}} - e\}$ to $\tau_{i,d(i)}^{\text{dr}} + \tau_{d(i),k}^{\text{dr}}$. For FSTSP we need to add $w_2 \max\{0, \tau_{i \rightarrow k}^{\text{tr}} + s_R + \sigma_k s_L - e\}$ to $\tau_{i \rightarrow k}^{\text{tr}} + s_R + \sigma_k s_L$ and add $w_2 \max\{0, \tau_{i,d(i)}^{\text{dr}} + \tau_{d(i),k}^{\text{dr}} + s_R - e\}$ to $\tau_{i,d(i)}^{\text{dr}} + \tau_{d(i),k}^{\text{dr}} + s_R$.

With the introduction of infeasibility considerations into Algorithm 3, it is noteworthy that the modifications exclusively impact the equation associated with $C_{\text{LL}}(i)$, leaving the overall structure of the algorithm unaltered. Consequently, the time complexity remains unchanged at $O(n^2)$, emphasizing the continued efficiency and scalability of the algorithm even in the presence of infeasible sequences.

Fitness evaluation

The optimal objective value, as determined by the JOIN algorithm, is the makespan obtained by the TSPD/FSTSP solution for a single feasible individual (penalized makespan if infeasible). In order to have greater diversity, the fitness measure will be calculated for each individual as a combination of the makespan (penalized makespan) and a diversity factor. Following Vidal et al. (2012), for two individuals P_1 and P_2 , a normalized Hamming distance $\delta^H(P_1, P_2)$ is defined as following:

$$\delta^H(P_1, P_2) = \frac{1}{n} \sum_{i=1}^n \mathbf{1}(P_1[i] \neq P_2[i]),$$

where $\mathbf{1}(\cdot)$ is equal to 1 if the condition specified within the parentheses is true and 0 otherwise, and n is the number of customers. The distance ranges between zero and one, with one indicating two individuals are completely different and zero indicating they are the same representation. The population is sorted according to the makespan determined by the JOIN algorithm, and diversity contribution $\Delta(P)$ is calculated by the average Hamming distance between an individual P and its two closest individuals within the population. According to the following formula, the fitness function for each individual is calculated:

$$\text{fitness}(P) = C_{\max}(P) \times \left(1 - \frac{n_{\text{ELITE}}}{n_{\text{POPULATION}}}\right)^{\Delta(P)},$$

where we let $C_{\max}(P)$ be the optimal makespan by the JOIN algorithm given individual P (and penalized makespan if P is infeasible), n_{ELITE} is the number of elite individuals and $n_{\text{POPULATION}}$ is the total number of individuals in the population.

This equation presents a nuanced modification compared to the formulation introduced by Vidal et al. (2012). In our adaptation, the diversity factor serves as the exponent, whereas in Vidal et al. (2012)'s work, it is employed as a multiplier.

4.4 Parent Selection, Crossover, and Mutation

During the crossover process, we select two parents, P_1 and P_2 , from which a new individual is produced. Various methods are available in the literature for selecting parents. For this study, we employ the *Tournament Selection* in which $k_{\text{TOURNAMENT}}$ individuals are randomly selected from the entire population, and the best one is selected as the parent based on fitness. A repeat of this process is conducted until two parents have been selected. It is important to note that before selecting parents, the entire population must be sorted according to fitness, introduced in Section 4.3, to accommodate diversity in the generation of offspring.

Several crossover methods designed for TSP for the generation of offspring exist in the literature. Having performed numerical experiments, we randomly employ four crossover methods, including Order Crossover (OX1) and Order-based Crossover (OX2) with minor modifications adapted to fit our problem and two crossovers designed specifically for TSPD in this study. Larranaga et al. (1999) contains details on these crossover methods, which is a review paper describing different representations and operators of GA for TSP. By creating two random crossover points in the parent, OX1 copies the segment between these crossover points to the offspring. From the second crossover point, the remaining unused numbers are copied from the second parent to the offspring in the same order in which they appear in the first parent. Upon reaching the end of the parent string, we begin at its first position. Using the OX2 operator, several positions in a parent string are randomly selected, and the ordered elements in the selected positions in this parent are imposed on the other parent. The elements missing from the offspring are added in the same order as in the second parent.

In our modification of OX1 and OX2, we perform these crossovers with absolute values and then

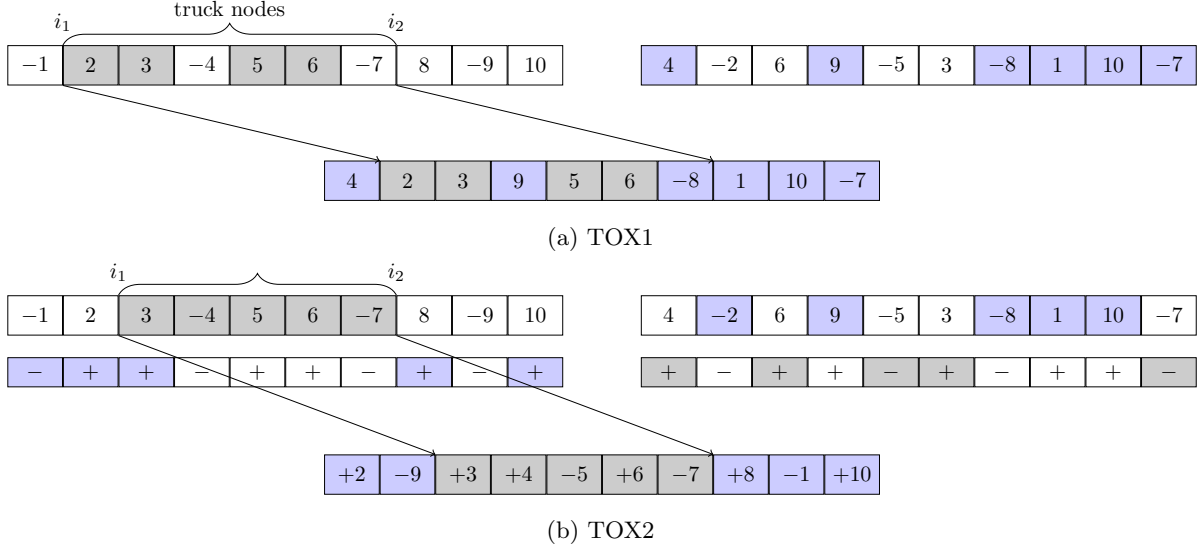


Figure 5: Examples of the type-aware order crossover operations, TOX1 and TOX2

retrieve the signs. This modification aims to capture both the order and the sign of nodes in the sequence. However, despite this enhancement, the resulting crossovers still fall short in fully addressing the unique attributes of TSPD, where the distinction between drone nodes and truck nodes is crucial.

To bridge this gap, we introduce two new crossover algorithms, collectively referred to as Type-Aware Order Crossover (TOX) methods. These methods are specifically tailored for TSPD and consider the different types of nodes present in the problem. In the first algorithm (TOX1), we begin by selecting either truck nodes or drone nodes from P_1 and copying the nodes between two randomly chosen indices to the offspring. The missing nodes are then added to the offspring in the order and type in which they appear in P_2 . In the second algorithm (TOX2), nodes from P_1 are copied into offspring between randomly selected nodes i_1 and i_2 , and the missing nodes are added in the order of P_2 . Afterward, the types (signs) of the nodes are determined based on P_2 for those between i_1 and i_2 , and based on P_1 for the remainder. We provide an example of TOX1 and TOX2 processes in Figure 5.

The motivation for developing TOX1 and TOX2 arises from the need to create crossovers that can capture the differences between drone nodes and truck nodes, ensuring that the offspring inherit all problem-specific properties from both parents. By considering the genetic attributes that determine the type of nodes as well as their sequence, TOX1 and TOX2 offer a more nuanced and problem-specific approach to crossover in the context of TSPD.

Empirical studies conducted across various problem domains utilizing GAs have substantiated the effectiveness of applying mutation on offspring. In our algorithm, once an offspring is produced, it undergoes mutation with a probability of P_M .

Two distinct mutation operators are randomly applied to the offspring: Sign Mutation and Tour Mutation.

Sign Mutation: This operator independently changes the sign of each element in the chromosome with a fixed probability of 0.1.

Tour Mutation: In this mutation scheme, 20 percent of the indices in the chromosome are randomly selected, and the elements at these positions are shuffled. This operation is analogous to the Scramble Mutation (Larranaga et al., 1999).

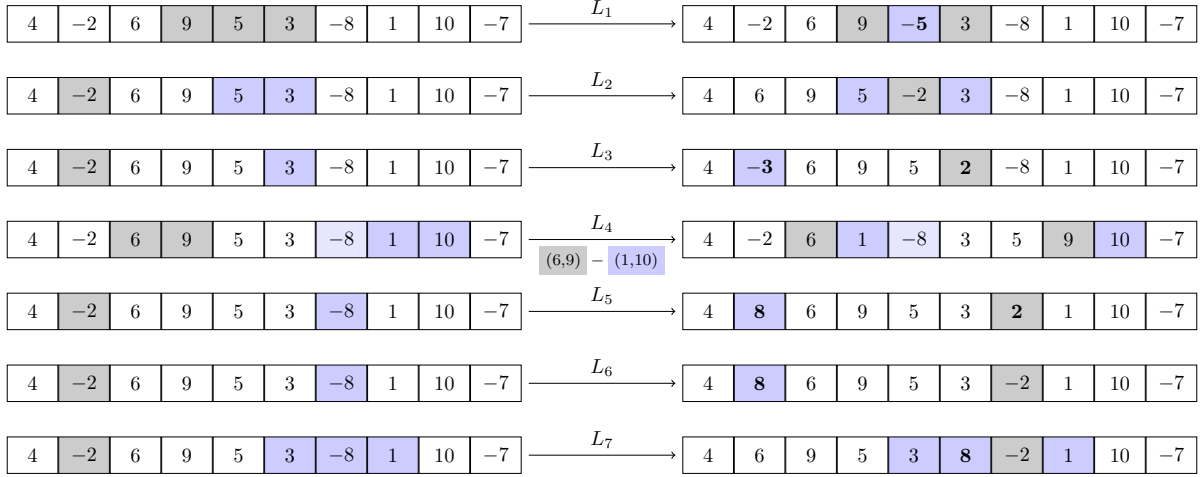


Figure 6: Illustration of L_1 to L_7 . The boldface means the type of the node is converted.

4.5 Improvement by Local Search

In contrast to the traditional GA, hybrid GA algorithms improve each offspring by local search. Ha et al. (2020) used sixteen local search neighborhoods specific to TSPD/FSTSP, which they call N_1 to N_{16} . Our study utilizes 15 of these neighborhoods N_1 to N_{15} . Since the neighborhood N_{16} is randomly modifying launch and rendezvous points for drone deliveries, it will not make any contributions because the JOIN algorithm is optimizing the launch and landing locations.

We introduce 7 new local search neighborhoods, labeled L_1 to L_7 , which are shown to make further improvements. A detailed description of these neighborhoods is provided below, and they are also illustrated in Figure 6. A numerical analysis is performed in Section 5.5 in order to evaluate the contribution of the new local search neighborhoods.

- L_1 , (Convert to drone): Randomly choose three consecutive truck nodes and convert the middle one to a drone node.
- L_2 , (Relocate a drone node): Remove a random drone node and randomly locate it between two consecutive truck nodes as a drone node.
- L_3 , (Swap truck-drone nodes): Choose a truck node and a drone node randomly and swap them while keeping the type of each position.
- L_4 , (Swap truck arcs): randomly select two arcs from the truck tour and swap them. The truck sequence as well as the drone sequence between the two arcs will be reversed.
- L_5 , (Swap drone nodes and convert both): Randomly choose two drone nodes and swap them while promoting their type to be truck nodes.
- L_6 , (Swap drone nodes and randomly convert one): Same as L_5 , only change the type of one node.
- L_7 , (Insert a drone node): Randomly choose a drone node d and a drone tuple $\langle i, j, k \rangle$, change j to truck node and insert d as either $\langle i, d, j, k \rangle$ or $\langle i, j, d, k \rangle$.

It is necessary to note that during the process of choosing the nodes randomly, we only select out of the n_{CLOSE} nearest ones, instead of all nodes, in order to save time. As previously indicated, following the generation of an offspring, a thorough evaluation for feasibility ensues. In the event that the offspring is deemed infeasible, with a probability denoted as P_{REPAIR} , a repair mechanism is invoked to rectify its

infeasibility, thereby rendering it feasible. The resulting feasible offspring is subsequently integrated into the feasible subpopulation. Conversely, an infeasible offspring is directed to the corresponding infeasible subpopulation based on the type of its infeasibility. For feasible offspring, an additional refinement step is introduced through the application of various local search neighborhoods, encompassing N_1 to N_{15} and L_1 to L_7 . The procedure involves sequentially applying each neighborhood to the offspring once, until an improvement occurs. Importantly, the order of neighborhood application is not fixed but rather undergoes random shuffling for every instance of offspring improvement. This approach ensures a diversified exploration of the solution space, contributing to the potential enhancement of the offspring's quality.

4.6 Population Management

A population management mechanism similar to that proposed in Vidal et al. (2012) is used in this study with one exception. Their study incorporates two subpopulations, feasible and infeasible. In our problem, there are three types of subpopulations: feasible, Type 1 infeasible (consecutive drone visits), and Type 2 infeasible (drone range violations). Subpopulations consist of at most $\mu + \lambda$ individuals, where μ denotes the minimum size of the subpopulation and λ represents the offspring pool size. Subpopulations are first initialized with size μ according to Algorithm 2. Each iteration will lead to the addition of the offspring to the corresponding subpopulation. Upon reaching the maximum size, λ individuals will be eliminated through a survivors selection process in order to reduce the population size back to μ . The top μ individuals are selected in accordance with makespan for feasible subpopulation and penalized makespan for infeasible subpopulations. Other important components of population management include penalty adjustment and diversification.

Penalty adjustment. During each iteration, the penalty parameters can be dynamically modified in order to control the type of offspring generated. The penalty parameters, w_1 and w_2 , are used in the JOIN algorithm and were defined in Section 4.3. We initialize the penalties with $w_1 = 2$ and $w_2 = 2$, and then update them during each iteration. Let ξ^{REF} be the target proportion of the feasible subpopulation size to the entire population size. In the case we have two infeasible subpopulations, their proportions will be maintained equally. Let ξ^F , ξ^M , and ξ^R denote the proportion of feasible, Type 1 and Type 2 infeasible subpopulations in the last 100 individuals generated, similar to Vidal et al. (2012). The following adjustment will be performed in every iteration:

- if $\xi^F < \xi^{REF} - \zeta$
 - if $\xi^R < \xi^M$, then $w_1 = \min\{\eta_I w_1, w_1^{\max}\}$
 - else $w_2 = \min\{\eta_I w_2, w_2^{\max}\}$
- if $\xi^F > \xi^{REF} + \zeta$
 - if $\xi^R < \xi^M$, then $w_2 = \max\{\eta_D w_2, w_2^{\min}\}$
 - else $w_1 = \max\{\eta_D w_1, w_1^{\min}\}$

where ζ is the tolerance level and η_I, η_D are multipliers to increase and decrease the penalty. We define w_1^{\max} and w_2^{\max} in order to prevent penalties from exploding, and w_1^{\min} and w_2^{\min} in order to prevent them from being smaller than 1.

Diversification. When no improvement is achieved after It_{DIV} iterations, we employ a plan to enhance the population’s genetic value. From each subpopulation, n_{BEST} individuals will be retained based on fitness, while the rest will be discarded. The size of each subpopulation will then reach μ using the same strategy as the initial population algorithm.

4.7 Escape Strategy

Typical meta-heuristic methods have the problem of solutions confined to a local optimal area, especially when local search is used, as in our algorithm. GAs offer a variety of tools for preventing premature convergence to local optima. Examples of such mechanisms include increasing population size and promoting diversification. It is noteworthy that while genetic variation can also be introduced through the process of mutation, this approach is inherently stochastic. Moreover, it is essential to underscore that the primary role of mutation in GAs is to prevent genetic drift rather than to solely address the premature convergence of the entire population. The complexity of the fitness function in TSPD, however, necessitates that we explore more intelligent and powerful methods for escaping the local optima. There is a possibility that the algorithm may be trapped in a local optimum point when it does not show any improvement over a certain number of iterations. The idea behind our trick is to generate a buffer of individuals with slightly poorer objective function values and then to randomly select one in each subsequent iteration and use local search to generate a better solution hoping it will escape the local optimum point. As our experiments demonstrated, this technique is very effective for escaping from local optima. Detailed information about this method can be found in Algorithm 4. The algorithm commences by initializing an empty list of individuals with a maximum capacity of n_{BUFFER} , adding the current population’s best individual to this buffer. Over the course of max_{iter} iterations, the algorithm performs the following operations. During each iteration, it randomly selects one individual from the buffer, chooses a local search neighborhood randomly, and applies a local search with the selected neighborhood to the chosen individual. If the modified individual surpasses the current best individual, it is added to the buffer, and the best individual is accordingly updated. Conversely, if the newly generated individual exhibits a larger makespan than the best individual, it is incorporated into the buffer only if the gap is smaller than a designated threshold denoted as ϵ_l . When adding a new individual to the buffer (Lines 10 and 13), it is simply added when the buffer is not full, and replaces the worst individual when it is full. Upon completion of the iterations, all individuals in the buffer that outperform the current population’s best individual are assimilated into the population. In our numerical experiments, we set $n_{BUFFER} = 40$, $\epsilon_l = 0.05$ and $max_{iter} = 10000$.

As previously stated, our proposed method is referred to as HGA-TAC. In instances where the escape strategy is applied, we denote the method as HGA-TAC⁺. Throughout our computational experiments, we address all problem instances both with and without the use of the escape strategy. Consequently, the reported results encompass both HGA-TAC and HGA-TAC⁺. In preparation for the subsequent section, we find it advantageous to provide a consolidated summary of all parameters employed in our approach across the paper. A comprehensive list of these parameters is presented in Table 1.

5 Computational Results

In this section, our focus is on assessing the effectiveness of our algorithm through experimentation on five widely recognized benchmark sets. First, we will outline the hardware and experimental settings as well as the parameters employed in the implementation of our algorithm and the methods applied for their refinement. Then, we will evaluate the effectiveness of HGA-TAC by comparing it to optimal solutions using randomly generated instances. Subsequently, we will provide a brief overview of the benchmark sets

Algorithm 4 Escaping from Local Optima

```
1:  $\omega_{\text{LOCAL}} \leftarrow \text{best}(\Omega_{\text{F}})$  ▷ local optimum point
2:  $\omega_{\text{BEST}} \leftarrow \omega_{\text{LOCAL}}$ 
3:  $\Omega_{\text{CANDIDATES}} \leftarrow \{\omega_{\text{BEST}}\}$  ▷ set of chromosomes
4: while number of iterations  $< \text{max}_{\text{iter}}$  do
5:   Randomly select  $\omega$  from  $\Omega_{\text{CANDIDATES}}$ 
6:   Randomly select  $L(\cdot)$  from the set of available local search neighborhoods
7:    $\omega' \leftarrow L(\omega)$ 
8:   if  $\omega' \notin \Omega_{\text{CANDIDATES}}$  then
9:     if  $C(\omega') < C(\omega_{\text{BEST}})$  then
10:      add  $\omega'$  to  $\Omega_{\text{CANDIDATES}}$ 
11:       $\omega_{\text{BEST}} \leftarrow \omega'$ 
12:     else if  $(C(\omega') - C(\omega_{\text{BEST}}))/C(\omega_{\text{BEST}}) < \epsilon_l$  then ▷  $\epsilon_l$  is a preset threshold.
13:       add  $\omega'$  to  $\Omega_{\text{CANDIDATES}}$ 
14:     end if
15:   end if
16: end while
17: for each  $\omega$  in  $\Omega_{\text{CANDIDATES}}$  do
18:   if  $C(\omega) < C(\omega_{\text{LOCAL}})$  then
19:      $\Omega_{\text{F}} \leftarrow \Omega_{\text{F}} \cup \{\omega\}$ 
20:   end if
21: end for
```

Table 1: A summarized list of all parameters used in this study. The last four parameters are only used in HGA-TAC⁺

Parameter	Description	Tuned Values
μ	Minimum size of each subpopulation	15
λ	Offspring pool size	25
$K_{\text{TOURNAMENT}}$	Number of randomly chosen individuals in parent selection procedure	5
n_{ELITE}	Parameter used in calculating fitness based on diversity factor	$0.2n_{\text{POPULATION}}$
n_{BEST}	Number of individuals retained during each implementation of diversification	0.3μ
P_{REPAIR}	Probability of repairing an infeasible generated offspring	0.5
P_M	Probability of mutation	0.1
ζ	Tolerance level in penalty adjustment procedure	0.05
η_I	Penalty increasing multiplier	1.1
η_D	Penalty decreasing multiplier	0.9
ξ^{REF}	Target proportion of the feasible individual generation	0.2
$w_1^{\text{max}}, w_1^{\text{min}}$	Maximum and minimum value allowed for penalty 1	8, 3
$w_2^{\text{max}}, w_2^{\text{min}}$	Maximum and minimum value allowed for penalty 2	5, 1.5
It_{NI}	The number of iterations with no improvements for stopping the algorithm	2500
It_{DIV}	The number of iterations with no improvements for performing the diversification	100
It_{LOC}	The number of iterations with no improvements for performing the escape strategy	1000
n_{BUFFER}	Maximum buffer size in escape strategy	40
ϵ_l	Threshold for accepting the new solution in escape strategy	0.05
max_{iter}	Maximum number of iterations in escape strategy	10000

utilized for comparative analysis. A comprehensive summary of all results will be presented in Tables 3 and 4. Following this, we will delve into a detailed examination of our algorithm’s performance on each benchmark set individually. For a more granular breakdown, please refer to the Appendix, where Tables 7-13 present the detailed results for each benchmark set.

5.1 Experimental conditions

The algorithm is coded and implemented in Julia programming language and is executed on a Mac computer with 16 GB of RAM and an Apple M1 processor. In the process of parameter tuning, we meticulously refined a significant portion of the parameters throughout the developmental phase of the algorithm. The refinement was a gradual and iterative process, closely aligned with the ongoing enhancements in the codebase. Specifically, for parameters μ , λ , n_{CLOSE} , and It_{DIV} , we employed a grid search methodology. This involved systematically exploring various combinations of these parameters using random samples extracted from diverse benchmark sets. The ultimate selection of parameter combinations was based on achieving the best results on average across these experiments. The values of all parameters utilized in this study after tuning are documented in Table 1.

Given the stochastic nature of GA, the outcomes may vary across individual runs on a specific instance. To ensure a comprehensive evaluation and equitable comparison with alternative methodologies, it is common practice to execute the algorithm multiple times and analyze the aggregated performance metrics. In this study, each instance is subjected to 10 independent runs, and the reported results encompass both the best and average outcomes derived from these 10 executions, respectively denoted as “Best” and “Avg.” in the tables.

5.2 Comparative Analysis with Exact Solutions

In preparation for evaluating our algorithm on established benchmark datasets, we conducted a preliminary examination of HGA-TAC’s accuracy on small-sized instances, where obtaining optimal solutions is feasible. To achieve this, we randomly generated small TSPD instances and solved them using the MILP formulation proposed by Roberti and Ruthmair (2021), implemented with Gurobi 9.5. The results were subsequently compared to those obtained by HGA-TAC. The random instance generation process involved selecting the depot location from a uniform distribution $[0, 1] \times [0, 1]$, while customer locations were chosen from a uniform distribution $[0, 10] \times [0, 10]$. Instances with 11, 12, and 13 customers were generated, with 10 instances for each size. These instances are publicly accessible in our GitHub repository.

Each of the 30 instances is solved with α values of 1, 2, and 3, representing the ratio of the drone’s speed to the truck’s speed, assuming an unlimited drone flying range. The computational times, measured in seconds, were recorded, and a time limit of 3600 seconds was set for MILP solutions. Table 6, which can be found in the appendix, summarizes the results for these 90 instances. The columns “Gap^b” and “Gap^a” denote the gap between the “Best” and “Avg.” results of HGA-TAC compared to the optimal solutions. It is noteworthy that HGA-TAC’s “Best” results were nearly equivalent in almost all instances (88 out of 90).

5.3 Benchmark sets

Our algorithm, tailored for addressing the TSPD and the FSTSP, undergoes rigorous evaluation across five meticulously chosen benchmark sets. These sets serve the dual purpose of assessing both TSPD and FSTSP instances, allowing for a comprehensive evaluation against state-of-the-art algorithms documented in the literature. The nomenclature of the benchmark sets in this study adheres to a systematic convention: The term ‘Set’ is followed by the initial character of the respective first author’s name from whose work

the sets are derived. The benchmark sets encompass a variety of scenarios, each strategically selected to enable robust comparisons. The TSPD benchmark sets utilize the Euclidean distance metric for both trucks and drones, while the FSTSP benchmark sets employ Manhattan and Euclidean metrics for trucks and drones, respectively. We consider the following benchmarks:

- **Set A_u :** Developed by Agatz et al. (2018), this set spans instances ranging from 10 to 250 nodes, designed to test TSPD with an unlimited drone flying range. Instances are categorized based on *uniform*, *single-center*, or *double-center* distributions. In uniform instances, the x and y coordinates for each location are independently and uniformly drawn from the set $\{1, 2, \dots, 100\}$, resulting in instances where the distribution of points is evenly spread across the available coordinate space. For single-center instances, each location follows a different approach. An angle a is uniformly drawn from the interval $[0, 2\pi]$, and a distance r is drawn from a normal distribution with a mean of 0 and a standard deviation of 50. The x coordinate of the location is then calculated as $r \cos a$, and the y coordinate is calculated as $r \sin a$. This methodology introduces a circular clustering effect, with locations concentrated around a central point. Double-center instances build upon the single-center concept. Similar to the single-center instances, locations are generated with an angle and distance. However, in this case, every location has a 50% chance of being translated by 200 distance units along the x -axis. This introduces a bimodal distribution, creating instances where locations are clustered around two distinct centers, adding an additional layer of complexity to the spatial arrangement. Each instance in this benchmark set is evaluated for three different values of α (the ratio of drone speed to truck speed: $\alpha \in \{1, 2, 3\}$). The set comprises 630 instances, and baseline algorithms for comparison include DPS/25 (Bogyrbayeva et al., 2023) and HGVNS (de Freitas and Penna, 2020).
- **Set A_l :** Also introduced by Agatz et al. (2018), this set focuses on TSPD with a limited drone flying range. Instances range from 10 to 100 nodes, with variations in drone range for each size. The uniform distribution is used for generating these instances. A total of 320 instances are included, and baseline algorithms for comparison are TSP-ep-all (Agatz et al., 2018) and DPS/25 (Bogyrbayeva et al., 2023).
- **Set B:** Created by Bogyrbayeva et al. (2023), this set consists of two subsets of TSPD instances with an unlimited drone range for $\alpha = 2$. The subsets, 'Random' and 'Amsterdam' differ in the method of instance generation. In the first subset of instances, a uniform distribution over $[0, 1] \times [0, 1]$ and $[0, 100] \times [0, 100]$ is used to sample the x and y coordinates of the depot and customer nodes, respectively. This makes the depot to be always located in the lower left corner. The method of generation is similar to that proposed by Agatz et al. (2018). For each size of 20, 50, and 100 nodes, 100 samples of instances are presented. The second subset of instances includes 100 samples for each size of 10, 20, and 50 nodes. The depot in this subset of instances, is randomly chosen out of the nodes. This benchmark set is chosen for its relevance in comparing our algorithm against the best existing Deep Reinforcement Learning (DRL) method for TSPD. Baseline algorithms include TSP-ep-all (Agatz et al., 2018), DPS/25, and the DRL-based Hybrid Model (HM) (Bogyrbayeva et al., 2023).
- **Set M:** Generated by Murray and Chu (2015), this FSTSP benchmark set comprises 36 instances with nodes distributed over an 8 miles by 8 miles area. Each instance includes 10 customers, of which 8 or 9 are eligible for drone visits. Using the Manhattan metric, the truck is assumed to be traveling at 25 miles per hour, and using the Euclidean distance metric, the drone is assumed to be traveling at 15, 25, or 35 miles per hour. Both the launch and retreat times, s_L and s_T , are set to one minute. The drone's endurance is either 20 or 40 minutes, which results in a total of 72

Table 2: A summary of the benchmark sets used in this study.

Benchmark Set	Problem	Size Range	Source Paper	Baseline Algorithms
Set A_u	TSPD	10 – 250	Agatz et al. (2018)	HGVNS, DPS/25
Set A_l	TSPD	10 – 100	Agatz et al. (2018)	TSP-ep-all, DPS/25
Set B	TSPD	10 – 100	Bogyrbayeva et al. (2023)	TSP-ep-all, DPS/25, HM
Set M	FSTSP	10	Murray and Chu (2015)	MC, HGA20
Set H	FSTSP	10 – 100	Ha et al. (2018)	HGA20

Table 3: A summary of results for HGA-TAC and HGA-TAC⁺ for all sets of instances. Time* means the time as reported in de Freitas and Penna (2020) for HGVNS, Ha et al. (2020) for HGA20 and Bogyrbayeva et al. (2023) for HM (4800). Computational times are measured in seconds.

Instance set	Baseline	DPS/25		HGA-TAC		HGA-TAC ⁺		Details (Section)
	Time*	Gap	Time	Gap	Time	Gap	Time	
TSPD	HGVNS							
Set A_u ($\alpha = 1$)	43.45	-10.45%	2.51	-10.66%	6.00	-11.14%	34.06	Table 7 (§5.5)
Set A_u ($\alpha = 2$)	41.16	-3.71%	4.78	-3.17%	8.32	-4.57%	45.98	Table 8 (§5.5)
Set A_u ($\alpha = 3$)	41.19	-1.20%	6.56	-2.07%	10.33	-4.15%	61.44	Table 9 (§5.5)
Set A_l	-	0.00%	0.50	0.07%	2.23	-0.52%	8.12	Table 10 (§5.5)
TSPD	HM (4800)							
Set B (rand)	2.07	1.02%	0.56	0.87%	2.18	-0.53%	8.16	Table 11 (§5.5)
Set B (Ams)	0.75	0.02%	0.22	-0.67%	0.69	-1.30%	2.29	Table 11 (§5.5)
FSTSP	HGA20							
Set M	-	-	-	-0.28%	0.40	-0.48%	1.16	Table 12 (§5.5)
Set H	159.60	-	-	-0.47%	3.60	-1.13%	16.20	Table 13 (§5.5)

instances. Baseline algorithms include Murray and Chu (2015)’s heuristic approach and HGA20 (Ha et al., 2020).

- **Set H:** Introduced by Ha et al. (2020), this set includes 60 instances with 10, 50, and 100 customers. Assumptions align with FSTSP by Murray and Chu (2015). The benchmark is designed for comparison with the HGA20 algorithm. Parameters include Manhattan distance for trucks, Euclidean distance for drones, and specific operational characteristics for both. Distance matrices are calculated using Manhattan distance for trucks and Euclidean distance for drones. The drone and truck have both been set to operate at a speed of 40 km/h. The drone is designed to fly for 20 minutes at a time. Launch time S_L and retrieval time S_R are both 1 minute and only 80% of the customers are eligible to be serviced by drones. This benchmark set is chosen to compare the performance of our algorithm with HGA20 (Ha et al., 2020).

A comprehensive overview of the features of these benchmark sets is provided in Table 2.

5.4 Summarized results

In Table 3, a concise summary of results is provided for all sets of instances, offering a high-level overview of the algorithmic performance. However, for a detailed examination of the outcomes for each set of instances, the reader is directed to Tables 7–13 in the Appendix. It is noteworthy that TSP-ep-all is exclusively utilized for sets A_u and B; therefore, its results are not included in this summary table. Instead, interested readers can refer to Tables 10 and 11 in the Appendix for a comprehensive analysis of TSP-ep-all outcomes. In the context of TSPD, sets A_u and A_l are segregated from set B due to differences

Table 4: Number of instances that HGA-TAC and HGA-TAC⁺ found the best solution for all sets of instances.

Instance set	Total	Better or equal				Strictly better			
		HGA-TAC		HGA-TAC ⁺		HGA-TAC		HGA-TAC ⁺	
		Best	Avg.	Best	Avg.	Best	Avg.	Best	Avg.
TSPD									
Set A _u ($\alpha = 1$)	210	160	124	202	164	114	82	153	120
Set A _u ($\alpha = 2$)	210	144	94	193	148	122	78	171	132
Set A _u ($\alpha = 3$)	210	186	130	209	184	165	116	188	169
Set A _l	320	222	163	262	202	75	47	115	74
Set B	600	426	250	536	361	308	183	423	284
TSPD Total	1550	1138	761	1402	1059	784	506	1050	779
FSTSP									
Set M	72	64	58	67	61	29	29	30	29
Set H	60	38	33	44	39	38	33	44	39
FSTSP Total	132	102	91	111	100	67	62	74	68
TOTAL	1682	1240	852	1513	1159	851	568	1124	847

in the primary baseline algorithm; for set A_u the primary baseline is HGVNS, whereas for set B the primary baseline is HM (4800). Furthermore, for the FSTSP results, DPS/25 is not applicable, as it is specifically designed for solving TSPD. The “Gap” is determined based on the average results obtained over 10 independent runs. Additionally, computational times for HGA20 on set M were not reported in Ha et al. (2020), leading to the absence of time-related information in Table 3. A cursory examination of the HGA-TAC⁺ column reveals competitive performance with acceptable computational times among the existing algorithms in the table.

Not only does our algorithm perform the best among available algorithms in the average sense, but it also finds the new best solutions for many benchmark instances. We report the number of instances in which our algorithms found a solution that was either equal to or better than the best existing solution. The results for each set of instances can be found in Table 4. The columns labeled “Best” and “Avg.” denote the number of instances where our algorithms’ best and average results (over 10 runs) are comparable with the best-known solutions, respectively. For example, in the last column of the first, “120” indicates that HGA-TAC⁺’s average results over 10 run are better than best-known solutions in 120 out of 210 instances. The detailed results for set A_u are compared only with those obtained by DPS/25. Thus, we cannot claim that our algorithms have found the best solutions, since running TSP-ep-all was not feasible due to the large problem sizes, and we did not have access to the detailed HGVNS results. Nevertheless, we have improved solutions in 512 out of 630 instances in comparison with DPS/25. Among the 320 examples of set A_l, our algorithms have demonstrated better or similar performance in 262 of them and strictly better performance in 115 of them, in terms of objective function. Based on 600 instances in set B our algorithms have found better or equal solutions in 536 instances and strictly better solutions in 423 instances, in terms of objective function. Excluding Set A_u, where results were compared only with DPS/25, a total of 920 TSPD instances from Sets A_l and B, where TSP-ep-all solutions were available, showed that our algorithms improved upon the best existing solutions in 538 instances. A similar performance can be observed for our algorithms when solving instances of FSTSP. Out of 72 instances of set M, we have found better or similar solutions in 67 instances and strictly better solutions in 30 instances. Out of 60 instances, 44 were improved by our algorithms for set H. As a result, we have found better solutions than the existing best for 74 of the 132 instances of FSTSP.

5.5 Detailed results

Results for the TSPD Instances with Unlimited Flying Range from Agatz et al. (2018)

In this section, we present a comprehensive analysis of the experiments conducted on set A_u , with detailed results provided in Tables 7, 8, and 9 for $\alpha = 1, 2$, and 3, respectively. These tables are available in the Appendix. To ensure a fair comparison, we have coded the DPS/25 in Julia and run it on the same machine. It is important to note, however, that the HGVNS method suggested by de Freitas and Penna (2020) was implemented in C++ and executed on a Core i7 processor with 3.6 GHz along with 16 GB of RAM. According to www.cpubenchmark.net, our processor is 2.52 times faster than theirs. HGVNS has an average run time of 41.93 seconds; however, after converting it to our processor performance, it will be 16.64 seconds, while HGA-TAC, HGA-TAC⁺, and DPS/25 have run times of 8.22, 47.16, and 1.11 seconds respectively. HGA-TAC is faster than HGVNS but slower than DPS/25. HGA-TAC has an average advantage of 5.30% over HGVNS and a 0.17% advantage over DPS/25. Where $\alpha = 2, 3$, HGA-TAC performs better than DPS/25, while DPS/25 provides better solutions when $\alpha = 1$. In spite of being slower, HGA-TAC⁺ shows an improvement of 6.62% and 1.51% over HGVNS and DPS/25, respectively. In all scenarios, HGA-TAC⁺ produces better solutions than DPS/25.

Results for the TSPD Instances with Limited Flying Ranges from Agatz et al. (2018)

The instances in set A_l are based on TSPD with restricted drone ranges. The results are summarized in Table 10 which can be found in the Appendix. The number of nodes in the instance is indicated in column N , and the ratio of drone range to the maximum distance between a pair of locations as a percentage is indicated in column r . Due to the fact that each drone operation involves traveling between two pairs of nodes, $r = 200$ indicates an unlimited flying range. We examine the effectiveness of our algorithm in this part by comparing the results with those of TSP-ep-all and DPS/25. In order to compare running times, all algorithms were developed in the same programming language (Julia) and executed on the same machine. As depicted in Table 10, HGA-TAC has better performance in instances with $n = 10$ and $n = 20$. In the case of $n = 50$, HGA-TAC is still outperforming DPS/25, in terms of solution quality. This is not the case in the rest of the sizes. HGA-TAC⁺, however, better objective function than DPS/25 in all cases. As compared to TSP-ep-all, averaged over all instances, HGA-TAC⁺ results in a 0.18% gap, where the average running time is 7.02 seconds, compared to 29.84 seconds for TSP-ep-all.

Results for the TSPD Instances from Bogrybayeva et al. (2023)

In this section, we present a comprehensive analysis of the experiments conducted on set B, with detailed results provided in Table 11 which can be found in the Appendix. The results of our HGA-TAC and HGA-TAC⁺ algorithms are compared to those obtained with TSP-ep-all, DPS/25, and HM (4800) in Bogrybayeva et al. (2023). HM stands for Hybrid Model based on deep reinforcement learning, and the HM (4800) represents the best solution generated by the neural network from 4800 samples. HGA-TAC and HGA-TAC⁺ have been run 10 times on each instance and we report the average and best results. The computational time for HGA-TAC(Best) and HGA-TAC⁺(Best) are obtainable by multiplying the corresponding run time by 10. TSP-ep-all and DPS/25 are implemented in our machine for a fair comparison of running time, while we present the time for HM (4800) reported in Bogrybayeva et al. (2023), implemented on NVIDIA A100 GPU (80 GiB) and AMD EPYC 7713 64-Core Processor CPU (128 threads used). Note, however, that training time is not included in the reported times for HM (4800).

For problems with a size smaller than 25, DPS/25 is identical to TSP-ep-all. Gaps are calculated in comparison with the results of TSP-ep-all as $\frac{(z - \bar{z})}{\bar{z}} \times 100$, where z and \bar{z} are the costs of each algorithm and TSP-ep-all respectively. For HGA-TAC and HGA-TAC⁺, the gaps are calculated based on the average values. Negative values for the gap indicate that the algorithm is outperforming TSP-ep-all. Among the algorithms, HGA-TAC⁺(Best) appears to perform the best on all instance sizes in both datasets. Compared to TSP-ep-all, HGA-TAC⁺(Avg.) shows better results in four of six cases and is slightly better overall. With instances of size 20, all of our algorithms outperform all other methods, in terms of solution quality. For larger sizes, however, the algorithms are in competition with one another over different cases.

Results for FSTSP instances from Murray and Chu (2015)

The next step is to test our algorithm using the FSTSP configuration. The results of our experiments on set M instances can be found in Table 12 in the Appendix. Using this collection of examples, we compare the performance of our method to that proposed by Murray and Chu (2015) as well as the HGA20 in Ha et al. (2020). In the same manner as HGA20, we solve each instance ten times and report both the best and average results. According to Table 12, our algorithms, HGA-TAC and HGA-TAC⁺, demonstrate significant improvements over existing methods, with respect to solution quality. There is no mention of computational times in either Murray and Chu (2015) or Ha et al. (2020). However, we provide the run times so that future comparisons can be made. In the column “Gap”, we indicate the difference between the average results of our method and those of HGA20. It is, however, the best of MC and HGA20-Best that we use to count the instances in which HGA-TAC and HGA-TAC⁺ have improved the existing solutions. As a result, HGA-TAC found better solutions in 29 instances and similar solutions in 35 instances. There were only 8 instances where it lost to the best baseline algorithm. Those numbers are 30, 37, and 5 for HGA-TAC⁺, respectively. Compared to HGA20, HGA-TAC and HGA-TAC⁺ show average performance improvements of 0.28% and 0.48%, respectively.

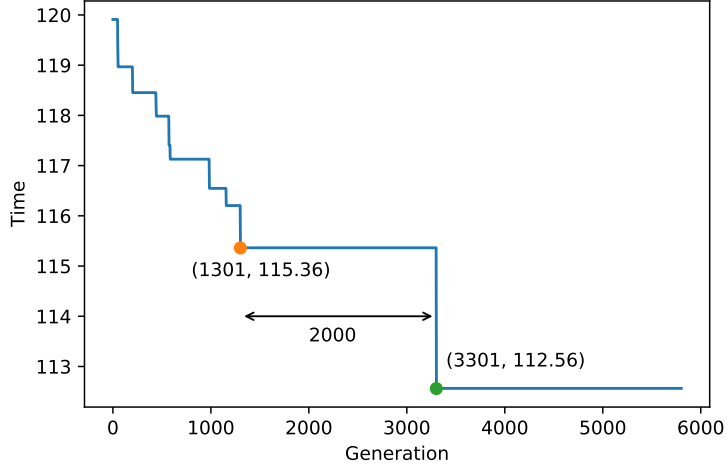
Results for FSTSP instances from Ha et al. (2018)

The results of our HGA-TAC and HGA-TAC⁺ on set H instances are compared in Table 13 (see Appendix) with HGA20 in Ha et al. (2020), which is implemented in C++ and executed on a desktop computer with an Intel Core i7-6700, 3.4 GHz processor. Based on the same scaling system in Section 5.5, their running times are comparable with ours if divided by 1.82. Each instance is solved 10 times, and the best and average solutions with the running time are reported. In the referenced paper, the times are reported in minutes, but we report them here in seconds. By scaling to our processor’s performance, the average running time for HGA20 is 87.60 seconds against 3.73 and 16.29 seconds for HGA-TAC and HGA-TAC⁺, respectively. HGA-TAC and HGA-TAC⁺, having 0.47% and 1.13% improvement over HGA20 solutions and being significantly faster, are clearly delivering superior results.

Moreover, the performance of L_1 – L_7 local search neighborhoods proposed in Section 4.5 has been evaluated by solving this set of problems with and without these neighborhoods. The results are presented in Table 5, in which the columns labeled “Best” and “Avg.” are obtained by taking an average over the makespan of all instances. The results indicate 0.45% and 0.81% improvement on average caused by our proposed neighborhoods in HGA-TAC and HGA-TAC⁺, respectively. We have included the average computational time for a fair comparison. Additionally, the column labeled “Improved” indicates the number of instances in which our results outperform those of HGA20. Notably, the introduction of new local search neighborhoods has contributed to the discovery of superior solutions in numerous instances within the dataset.

Table 5: Contributions of new local search neighborhoods L_1-L_7

FSTSP Set H	without L_1-L_7				with L_1-L_7			
	Best	Avg.	Time	Improved	Best	Avg.	Time	Improved
HGA-TAC	261.66	263.55	3.13	31	260.66	262.37	3.37	38
HGA-TAC ⁺	260.74	262.92	14.65	37	258.92	260.85	16.29	44

Figure 7: The objective function of instance B6 over generations, solved by HGA-TAC⁺. The final solution found by HGA-TAC⁺ is 112.56.

5.6 The effectiveness of the Escape Strategy

This section aims to illustrate the effectiveness of the escape local optima plan. As stated previously, every 1000 iterations without any improvement, Algorithm 4 is triggered and attempts to escape the local optimum point. A detailed representation of the instance B6 chosen from FSTSP Set H, as solved by HGA-TAC⁺, is shown in Figure 7. After generation 1301, the GA appears to be trapped in the local optima with an objective value of 115.36. However, at the second attempt to escape the local optima, the algorithm manages to obtain an objective value of 112.56. This was an example of what happens behind the scenes of the HGA-TAC⁺ algorithm compared to the regular HGA-TAC algorithm.

To assess the effectiveness of the Escape Strategy, we employed instances from Set A_u . For this analysis, we solved instances of sizes 20, 50, 75, 100, 175, and 250, employing both HGA-TAC and HGA-TAC⁺. Each instance size, represented as a graph in Figure 8, encompasses 90 instances derived from three distributions and three alpha values, with 10 instances per setting. To gauge the convergence behavior, we calculated the average relative gap over these instances. Initially, we standardized the iteration counts across all instances by interpolating the data and dividing the values by the best objective value found by HGA-TAC⁺, ensuring uniformity in the number of iterations and a comparable scale among different instances. Subsequently, we computed the average gap across the instances within each group. Upon analysis of Figure 8, it is evident that the Escape Strategy exhibits minimal impact on instances of size 20. This observation suggests that HGA-TAC already attains near-optimal solutions for smaller instances, leaving limited room for further improvement. However, as the instance sizes increase, the Escape Strategy demonstrates a pronounced effect, notably enhancing the Makespan at the expense of additional iterations.

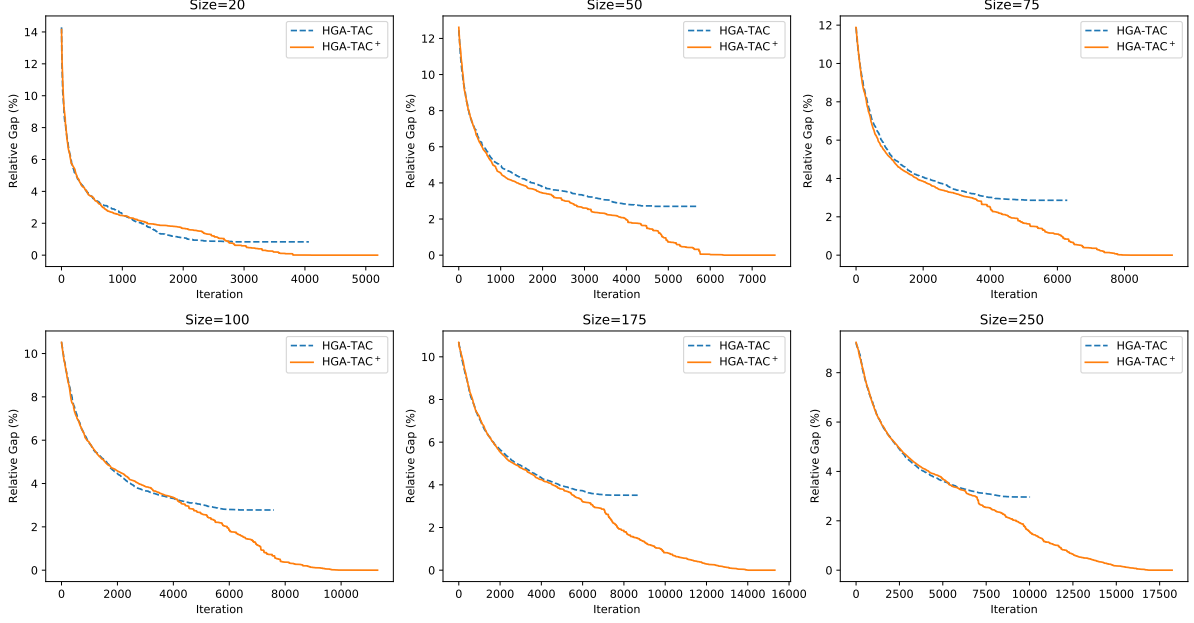


Figure 8: Evaluating the effectiveness of the Escape Strategy using benchmark set A_u .

6 Conclusions

This paper presented a Hybrid Genetic Algorithm with Type-Aware Chromosome encoding (HGA-TAC), to solve TSPD and FSTSP. The GA is responsible for partitioning and managing the sequences of the customers, while the DP is responsible for determining the rendezvous points and calculating the objective value. TSPD and FSTSP both aim to find the best routes for trucks and drones, yet several assumptions differ slightly between the two. There were several local search neighborhoods offered, along with two crossover approaches that were specifically designed for our problem.

A key innovation presented in this work is the “escape strategy,” detailed in Section 4.7, which effectively addresses the challenge of local optima inherent in meta-heuristic methods. The “escape strategy” serves as a versatile tool for diversification within GAs, transcending the confines of our specific problem. By generating a buffer of individuals and strategically applying local search, the algorithm escapes local optima, contributing to improved solution quality. This strategy, outlined in Algorithm 4, has proven effective across various scenarios, as demonstrated in our numerical experiments. The adaptability of the “escape strategy” suggests its potential as a general diversification method for Genetic Algorithms, offering a promising avenue for future research.

As evidenced by our testing on five benchmark sets of instances, our GA either exceeded or was competitive with the best existing methods. We believe the faster performance in our method is due to making the decisions about the sequence and node types by GA and leaving less information to be decided optimally by DP. Moreover, it was observed that Escape Strategy improved the quality of the solution at the cost of increased running time.

A few future research directions may be considered. A generalized version of the proposed method can be implemented using multiple drones in conjunction with a truck in order to solve the TSPD. A further extension could involve allowing the drone to visit more than one customer in a single operation. Furthermore, the proposed method in this paper could be extended to vehicle routing problems with drones, where a fleet of multiple trucks and multiple drones is routed.

Acknowledgment

This material is based upon work supported by the National Research Foundation of Korea (NRF) grant funded by the Korean government (MSIT) [Grant No. RS-2023-00259550] and by the National Science Foundation [Grant No. 2032458].

References

- Agatz, N., P. Bouman, M. Schmidt. 2018. Optimization approaches for the traveling salesman problem with drone. *Transportation Science* **52**(4) 965–981.
- Baldacci, R., A. Mingozzi, R. Roberti. 2011. New route relaxation and pricing strategies for the vehicle routing problem. *Operations Research* **59**(5) 1269–1283.
- Boccia, M., A. Masone, A. Sforza, C. Sterle. 2021. A column-and-row generation approach for the flying sidekick travelling salesman problem. *Transportation Research Part C: Emerging Technologies* **124** 102913.
- Bogyrbayeva, A., T. Yoon, H. Ko, S. Lim, H. Yun, C. Kwon. 2023. A deep reinforcement learning approach for solving the traveling salesman problem with drone. *Transportation Research Part C: Emerging Technologies* 103981.
- Bouman, P., N. Agatz, M. Schmidt. 2018. Dynamic programming approaches for the traveling salesman problem with drone. *Networks* **72**(4) 528–542.
- Campuzano, G., E. Lalla-Ruiz, M. Mes. 2021. A multi-start vns algorithm for the tsp-d with energy constraints. *International Conference on Computational Logistics*. Springer, 393–409.
- Chung, S. H., B. Sah, J. Lee. 2020. Optimization for drone and drone-truck combined operations: A review of the state of the art and future directions. *Computers & Operations Research* **123** 105004.
- de Freitas, J. C., P. H. V. Penna. 2020. A variable neighborhood search for flying sidekick traveling salesman problem. *International Transactions in Operational Research* **27**(1) 267–290.
- Ferrandez, S. M., T. Harbison, T. Weber, R. Sturges, R. Rich. 2016. Optimization of a truck-drone in tandem delivery network using k-means and genetic algorithm. *Journal of Industrial Engineering and Management* **9**(2) 374–388.
- Ha, Q. M., Y. Deville, Q. D. Pham, M. H. Hà. 2018. On the min-cost traveling salesman problem with drone. *Transportation Research Part C: Emerging Technologies* **86** 597–621.
- Ha, Q. M., Y. Deville, Q. D. Pham, M. H. Hà. 2020. A hybrid genetic algorithm for the traveling salesman problem with drone. *Journal of Heuristics* **26**(2) 219–247.
- Helsgaun, K. 2000. An effective implementation of the lin–kernighan traveling salesman heuristic. *European Journal of Operational Research* **126**(1) 106–130.
- Ho, W., G. T. Ho, P. Ji, H. C. Lau. 2008. A hybrid genetic algorithm for the multi-depot vehicle routing problem. *Engineering Applications of Artificial Intelligence* **21**(4) 548–557.
- Larranaga, P., C. M. H. Kuijpers, R. H. Murga, I. Inza, S. Dizdarevic. 1999. Genetic algorithms for the travelling salesman problem: A review of representations and operators. *Artificial Intelligence Review* **13** 129–170.

- Li, H., J. Chen, F. Wang, M. Bai. 2021. Ground-vehicle and unmanned-aerial-vehicle routing problems from two-echelon scheme perspective: A review. *European Journal of Operational Research* **294**(3) 1078–1095.
- Lin, S., B. W. Kernighan. 1973. An effective heuristic algorithm for the traveling-salesman problem. *Operations Research* **21**(2) 498–516.
- Luo, Z., M. Poon, Z. Zhang, Z. Liu, A. Lim. 2021. The multi-visit traveling salesman problem with multi-drones. *Transportation Research Part C: Emerging Technologies* **128** 103172.
- Macrina, G., L. D. P. Pugliese, F. Guerriero, G. Laporte. 2020. Drone-aided routing: A literature review. *Transportation Research Part C: Emerging Technologies* **120** 102762.
- Moscato, P., et al. 1989. On evolution, search, optimization, genetic algorithms and martial arts: Towards memetic algorithms. *Caltech concurrent computation program, C3P Report* **826**(1989) 37.
- Murray, C. C., A. G. Chu. 2015. The flying sidekick traveling salesman problem: Optimization of drone-assisted parcel delivery. *Transportation Research Part C: Emerging Technologies* **54** 86–109.
- Otto, A., N. Agatz, J. Campbell, B. Golden, E. Pesch. 2018. Optimization approaches for civil applications of unmanned aerial vehicles (UAVs) or aerial drones: A survey. *Networks* **72**(4) 411–458.
- Poikonen, S., B. Golden, E. A. Wasil. 2019. A branch-and-bound approach to the traveling salesman problem with a drone. *INFORMS Journal on Computing* **31**(2) 335–346.
- Roberti, R., M. Ruthmair. 2021. Exact methods for the traveling salesman problem with drone. *Transportation Science* **55**(2) 315–335.
- Vidal, T., T. G. Crainic, M. Gendreau, N. Lahrichi, W. Rei. 2012. A hybrid genetic algorithm for multidepot and periodic vehicle routing problems. *Operations Research* **60**(3) 611–624.
- Yang, Y., C. Yan, Y. Cao, R. Roberti. 2023. Planning robust drone-truck delivery routes under road traffic uncertainty. *European Journal of Operational Research* **309**(3) 1145–1160.

Appendix: Tables representing the details of experiments

Table 6: Evaluation of HGA-TAC against optimal solutions for randomly generated instances

		$\alpha = 1$							$\alpha = 2$							$\alpha = 3$						
N	Ins.	MILP		HGA-TAC					MILP		HGA-TAC					MILP		HGA-TAC				
		Obj	Time	Best	Avg.	Time	Gap ^b	Gap ^a	Obj	Time	Best	Avg.	Time	Gap ^b	Gap ^a	Obj	Time	Best	Avg.	Time	Gap ^b	Gap ^a
11	1	26.242	24.40	26.242	26.242	0.52	0.00%	0.00%	22.883	21.20	22.883	22.913	0.31	0.00%	0.13%	20.260	5.69	20.260	20.767	0.27	0.00%	2.50%
	2	26.652	140.67	26.652	26.890	0.45	0.00%	0.89%	21.889	22.35	21.889	22.206	0.22	0.00%	1.45%	21.251	21.11	21.251	21.511	0.29	0.00%	1.22%
	3	25.289	11.98	25.289	25.289	0.34	0.00%	0.00%	19.996	11.22	19.996	19.996	0.28	0.00%	0.00%	17.339	4.79	17.339	17.339	0.26	0.00%	0.00%
	4	24.084	18.49	24.084	24.084	0.32	0.00%	0.00%	18.784	18.51	18.789	19.013	0.34	0.03%	1.22%	15.455	6.24	15.455	15.741	0.27	0.00%	1.85%
	5	24.685	11.44	24.685	24.685	0.31	0.00%	0.00%	19.703	3.67	19.703	19.715	0.28	0.00%	0.06%	18.210	3.86	18.210	18.210	0.24	0.00%	0.00%
	6	24.877	58.00	24.877	24.877	0.34	0.00%	0.00%	19.630	25.58	19.630	19.643	0.25	0.00%	0.07%	17.200	21.63	17.200	17.307	0.25	0.00%	0.62%
	7	26.432	27.97	26.432	26.432	0.43	0.00%	0.00%	22.749	17.81	22.749	22.757	0.29	0.00%	0.03%	19.118	6.52	19.118	19.484	0.28	0.00%	1.91%
	8	27.436	317.87	27.436	27.436	0.35	0.00%	0.00%	20.903	29.41	20.903	20.903	0.27	0.00%	0.00%	17.842	21.01	17.842	17.842	0.23	0.00%	0.00%
	9	30.635	37.28	30.635	30.635	0.32	0.00%	0.00%	27.035	17.41	27.035	27.065	0.28	0.00%	0.11%	25.781	28.28	25.781	25.855	0.24	0.00%	0.29%
	10	28.357	99.15	28.357	28.357	0.36	0.00%	0.00%	23.195	32.01	23.195	23.195	0.30	0.00%	0.00%	21.609	20.82	21.609	21.679	0.20	0.00%	0.32%
Average		26.469	74.73	26.469	26.493	0.37	0.00%	0.09%	21.677	19.92	21.677	21.741	0.28	0.00%	0.31%	19.407	13.99	19.407	19.574	0.25	0.00%	0.87%
12	1	27.133	201.41	27.133	27.133	0.37	0.00%	0.00%	23.565	78.46	23.565	23.570	0.33	0.00%	0.02%	21.175	41.42	21.175	21.312	0.31	0.00%	0.65%
	2	31.016	98.31	31.016	31.016	0.41	0.00%	0.00%	26.835	32.80	26.835	27.066	0.29	0.00%	0.86%	24.406	28.92	24.406	25.891	0.24	0.00%	6.09%
	3	30.006	145.84	30.006	30.006	0.35	0.00%	0.00%	25.563	61.74	25.563	25.586	0.35	0.00%	0.09%	22.307	25.65	22.307	22.340	0.28	0.00%	0.15%
	4	27.424	151.74	27.424	27.450	0.54	0.00%	0.10%	24.091	87.07	24.091	24.110	0.33	0.00%	0.08%	19.934	22.31	19.934	20.574	0.30	0.00%	3.21%
	5	29.300	143.54	29.300	29.300	0.36	0.00%	0.00%	23.188	50.54	23.188	23.188	0.39	0.00%	0.00%	20.187	38.50	20.233	20.664	0.29	0.23%	2.36%
	6	32.602	271.05	32.602	32.602	0.49	0.00%	0.00%	26.706	61.07	26.706	26.706	0.21	0.00%	0.00%	24.091	33.01	24.091	24.091	0.26	0.00%	0.00%
	7	25.553	100.30	25.553	25.553	0.37	0.00%	0.00%	20.817	31.99	20.817	20.817	0.24	0.00%	0.00%	18.424	16.27	18.424	18.990	0.28	0.00%	3.07%
	8	26.165	989.88	26.165	26.448	0.48	0.00%	1.08%	20.020	46.61	20.020	20.052	0.42	0.00%	0.16%	17.951	40.99	17.951	17.952	0.29	0.00%	0.01%
	9	26.734	63.29	26.734	26.734	0.35	0.00%	0.00%	24.185	32.99	24.185	24.185	0.21	0.00%	0.00%	23.488	28.64	23.488	23.587	0.24	0.00%	0.42%
	10	27.502	135.34	27.502	27.502	0.37	0.00%	0.00%	22.751	37.73	22.751	23.186	0.26	0.00%	1.91%	20.028	26.54	20.028	20.538	0.24	0.00%	2.55%
Average		28.344	230.07	28.344	28.374	0.41	0.00%	0.12%	23.772	52.10	23.772	23.847	0.30	0.00%	0.31%	21.199	30.22	21.204	21.594	0.27	0.02%	1.85%
13	1	28.928	702.75	28.928	28.928	0.41	0.00%	0.00%	22.928	161.79	22.928	23.451	0.37	0.00%	2.28%	22.201	119.34	22.201	22.361	0.36	0.00%	0.72%
	2	28.248	216.68	28.248	28.248	0.43	0.00%	0.00%	23.399	218.65	23.399	23.399	0.31	0.00%	0.00%	20.166	54.59	20.166	20.264	0.37	0.00%	0.49%
	3	24.801	66.32	24.801	24.801	0.40	0.00%	0.00%	20.049	120.03	20.049	20.197	0.41	0.00%	0.74%	17.662	158.24	17.662	17.662	0.31	0.00%	0.00%
	4	29.880	1922.53	29.880	29.880	0.40	0.00%	0.00%	24.323	126.63	24.323	24.323	0.32	0.00%	0.00%	22.252	98.20	22.252	22.989	0.32	0.00%	3.32%
	5	28.477	3424.74	28.477	28.504	0.55	0.00%	0.09%	22.563	333.62	22.563	22.629	0.39	0.00%	0.30%	19.438	115.44	19.438	19.447	0.33	0.00%	0.05%
	6	31.222	826.71	31.222	31.222	0.41	0.00%	0.00%	24.879	163.55	24.879	24.879	0.35	0.00%	0.00%	22.478	52.41	22.478	22.650	0.29	0.00%	0.76%
	7	29.634	1644.62	29.635	29.635	0.39	0.00%	0.00%	22.844	149.30	22.844	23.175	0.46	0.00%	1.45%	20.505	66.75	20.505	20.748	0.28	0.00%	1.19%
	8	32.879	74.07	32.879	32.885	0.50	0.00%	0.02%	27.415	98.86	27.415	27.437	0.32	0.00%	0.08%	25.166	115.05	25.166	25.220	0.33	0.00%	0.22%
	9	27.076	2099.43	27.076	27.076	0.39	0.00%	0.00%	22.698	1232.83	22.698	23.145	0.46	0.00%	1.97%	18.647	88.85	18.647	18.808	0.35	0.00%	0.87%
	10	31.129	3600.02	31.129	31.210	0.53	0.00%	0.26%	24.964	1207.84	24.964	25.126	0.31	0.00%	0.65%	23.710	207.95	23.710	23.779	0.24	0.00%	0.29%
Average		29.227	1457.79	29.228	29.239	0.44	0.00%	0.04%	23.606	381.31	23.606	23.776	0.37	0.00%	0.75%	21.222	107.68	21.222	21.393	0.32	0.00%	0.79%

Table 7: (TSPD Set A_u, $\alpha = 1$) Results of HGA-TAC and HGA-TAC⁺ for Agatz et al. (2018) instances with $\alpha = 1$. Times are in seconds, and Time* is as reported in de Freitas and Penna (2020).

Dist	N	HGVNS		DPS/25		HGA-TAC		Gap Over (%)		HGA-TAC ⁺		Gap Over (%)	
		Obj	Time*	Obj	Time	Avg.	Time	HGVNS	DPS/25	Avg.	Time	HGVNS	DPS/25
Uniform	10	289.82	0.14	265.20	0.01	265.20	0.23	−8.49	0.00	265.20	0.70	−8.49	0.00
	20	368.54	0.11	325.23	0.06	326.40	0.49	−11.43	0.36	324.76	1.78	−11.88	−0.15
	50	559.20	3.71	498.20	0.26	498.45	1.55	−10.86	0.05	493.84	6.54	−11.69	−0.87
	75	624.32	16.30	574.21	0.39	576.40	2.66	−7.68	0.38	572.61	11.50	−8.28	−0.28
	100	698.42	53.50	655.87	0.54	659.41	3.89	−5.59	0.54	652.00	19.29	−6.65	−0.59
	175	905.32	55.91	841.39	1.56	843.36	9.27	−6.84	0.23	837.72	48.17	−7.47	−0.44
	250	1135.32	185.19	988.59	2.26	982.64	21.33	−13.45	−0.60	978.43	112.67	−13.82	−1.03
	Average		44.98		0.73		5.63	−9.19	0.14		28.66	−9.75	−0.48
Single Center	10	364.92	0.13	335.29	0.01	335.27	0.21	−8.12	0.00	335.27	0.70	−8.12	0.00
	20	553.53	0.85	462.1	0.06	458.74	0.51	−17.13	−0.73	458.30	1.84	−17.20	−0.82
	50	784.32	2.30	657.79	0.27	654.67	2.06	−16.53	−0.47	650.62	8.68	−17.05	−1.09
	75	978.32	10.93	890.12	0.48	884.49	3.02	−9.59	−0.63	878.59	14.74	−10.19	−1.30
	100	1193.95	37.77	1065.77	0.57	1061.36	5.25	−11.10	−0.41	1053.90	23.25	−11.73	−1.11
	175	1629.32	39.28	1420.95	1.31	1421.04	11.45	−12.78	0.01	1412.82	68.86	−13.29	−0.57
	250	1813.54	191.48	1646.00	1.94	1645.99	18.61	−9.24	0.00	1636.44	146.19	−9.77	−0.58
	Average		40.39		0.66		5.87	−12.07	−0.32		37.75	−12.48	−0.78
Double Center	10	634.42	0.14	586.6	0.01	586.60	0.20	−7.54	0.00	586.60	0.66	−7.54	0.00
	20	754.81	0.11	709.79	0.08	711.46	0.50	−5.74	0.23	711.58	1.73	−5.73	0.25
	50	1203.09	3.71	1010.88	0.28	1002.62	2.08	−16.66	−0.82	993.95	8.05	−17.38	−1.67
	75	1494.57	16.30	1243.47	0.43	1239.43	3.66	−17.07	−0.32	1229.48	15.58	−17.74	−1.13
	100	1556.52	53.50	1405.57	0.59	1393.82	5.23	−10.45	−0.84	1383.34	24.02	−11.13	−1.58
	175	2072.36	55.91	1910.03	1.22	1912.26	12.92	−7.73	0.12	1898.27	65.24	−8.40	−0.62
	250	2523.00	185.19	2275.4	1.77	2273.47	20.96	−9.89	−0.08	2263.12	135.06	−10.30	−0.54
	Average		44.98		0.63		6.51	−10.73	−0.24		35.76	−11.17	−0.76

Table 8: (TSPD Set A_u , $\alpha = 2$) Results of HGA-TAC and HGA-TAC⁺ for Agatz et al. (2018) instances with $\alpha = 2$. Times are in seconds, and Time* is as reported in de Freitas and Penna (2020).

Dist	N	HGVNS		DPS/25		HGA-TAC		Gap Over (%)		HGA-TAC ⁺		Gap Over (%)	
		Obj	Time*	Obj	Time	Avg.	Time	HGVNS	DPS/25	Avg.	Time	HGVNS	DPS/25
Uniform	10	233.20	0.13	218.57	0.01	218.04	0.17	-6.50	-0.24	218.08	0.54	-6.49	-0.22
	20	293.60	0.85	277.51	0.11	274.87	0.36	-6.38	-0.95	274.19	1.25	-6.61	-1.20
	50	420.80	2.30	420.60	0.59	415.69	1.38	-1.21	-1.17	408.00	4.96	-3.04	-2.99
	75	490.43	10.93	482.16	0.81	484.13	2.77	-1.28	0.41	473.58	9.99	-3.44	-1.78
	100	553.43	37.77	559.52	1.06	564.05	4.54	1.92	0.81	551.17	17.36	-0.41	-1.49
	175	704.53	39.28	711.85	2.91	724.53	13.10	2.84	1.78	703.67	70.72	-0.12	-1.15
	250	824.42	191.48	837.04	3.21	850.17	26.93	3.12	1.57	827.24	202.02	0.34	-1.17
	Average		40.39		1.24		7.03	-1.07	0.32		43.83	-2.82	-1.43
Single Center	10	291.36	0.14	261.61	0.01	260.33	0.18	-10.65	-0.49	260.40	0.61	-10.63	-0.46
	20	364.08	1.04	351.06	0.09	352.55	0.42	-3.17	0.42	349.54	1.57	-3.99	-0.43
	50	593.54	2.23	521.66	0.55	515.72	1.57	-13.11	-1.14	510.63	4.86	-13.97	-2.12
	75	754.43	11.18	715.27	0.90	712.99	3.28	-5.49	-0.32	703.45	10.43	-6.76	-1.65
	100	900.12	38.23	858.12	1.10	873.27	5.39	-2.98	1.77	856.52	19.53	-4.84	-0.19
	175	1183.43	43.06	1157.29	2.09	1178.93	16.22	-0.38	1.87	1156.92	78.61	-2.24	-0.03
	250	1294.43	197.12	1339.34	3.46	1375.14	36.45	6.24	2.67	1347.80	214.73	4.12	0.63
	Average		41.86		1.17		9.07	-4.22	0.68		47.19	-5.47	-0.61
Double Center	10	510.09	0.13	467.14	0.01	465.00	0.16	-8.84	-0.46	464.97	0.55	-8.85	-0.46
	20	605.04	0.98	590.99	0.12	587.47	0.40	-2.90	-0.60	586.89	1.31	-3.00	-0.69
	50	850.31	2.24	825.09	0.49	813.72	1.71	-4.30	-1.38	800.86	5.52	-5.82	-2.94
	75	1123.61	11.61	1018.52	0.85	1012.58	3.57	-9.88	-0.58	994.88	11.76	-11.46	-2.32
	100	1199.09	38.22	1138.35	1.11	1153.25	6.05	-3.82	1.31	1139.70	20.22	-4.95	0.12
	175	1659.37	42.31	1568.74	2.11	1601.50	16.21	-3.49	2.09	1567.70	76.79	-5.52	-0.07
	250	1862.44	193.17	1862.93	3.03	1931.15	33.94	3.69	3.66	1894.26	212.31	1.71	1.68
	Average		41.24		1.10		8.86	-4.22	0.58		46.92	-5.41	-0.67

Table 9: (TSPD Set A_u , $\alpha = 3$) Results of HGA-TAC and HGA-TAC⁺ for Agatz et al. (2018) instances with $\alpha = 3$. Times are in seconds, and Time* is as reported in de Freitas and Penna (2020).

Dist	N	HGVNS		DPS/25		HGA-TAC		Gap Over (%)		HGA-TAC ⁺		Gap Over (%)	
		Obj	Time*	Obj	Time	Avg.	Time	HGVNS	DPS/25	Avg.	Time	HGVNS	DPS/25
uniform	10	215.88	0.13	203.32	0.01	198.70	0.15	-7.96	-2.28	198.97	0.51	-7.83	-2.14
	20	274.20	1.15	256.18	0.14	252.45	0.35	-7.93	-1.46	252.63	1.11	-7.87	-1.39
	50	389.80	2.19	393.12	0.73	385.36	1.37	-1.14	-1.98	375.70	4.48	-3.62	-4.43
	75	447.64	10.95	454.50	0.97	448.65	2.95	0.23	-1.29	433.19	10.58	-3.23	-4.69
	100	510.20	37.26	530.17	1.43	524.85	5.45	2.87	-1.00	509.00	18.25	-0.23	-3.99
	175	655.20	41.49	670.67	3.78	674.81	15.78	2.99	0.62	646.13	91.43	-1.38	-3.66
	250	758.32	189.43	792.99	4.18	801.46	33.30	5.69	1.07	765.79	268.35	0.98	-3.43
	Average		40.37		1.61		8.48	-0.75	-0.90		56.39	-3.31	-3.39
Single center	10	242.20	0.13	224.38	0.01	219.86	0.15	-9.22	-2.01	219.71	0.53	-9.29	-2.08
	20	319.80	0.86	295.93	0.15	293.13	0.39	-8.34	-0.95	291.33	1.33	-8.90	-1.55
	50	493.43	2.19	471.78	0.71	452.29	1.67	-8.34	-4.13	442.38	5.09	-10.35	-6.23
	75	638.20	11.39	647.68	1.23	635.32	3.92	-0.45	-1.91	619.76	10.70	-2.89	-4.31
	100	804.43	37.74	777.00	1.47	772.90	6.50	-3.92	-0.53	759.03	21.32	-5.64	-2.31
	175	998.53	41.20	1048.29	2.71	1063.19	21.44	6.48	1.42	1030.37	95.83	3.19	-1.71
	250	1224.43	198.72	1233.68	3.94	1241.86	44.01	1.42	0.66	1206.40	300.99	-1.47	-2.21
	Average		41.75		1.46		11.15	-3.20	-1.06		62.26	-5.05	-2.92
Double Center	10	439.60	0.13	421.94	0.01	413.14	0.15	-6.02	-2.08	413.14	0.51	-6.02	-2.08
	20	586.74	0.99	560.54	0.14	548.91	0.37	-6.45	-2.07	548.11	1.06	-6.58	-2.22
	50	746.93	2.14	760.15	0.71	739.64	1.60	-0.98	-2.70	726.96	4.64	-2.67	-4.37
	75	945.34	11.22	934.53	1.01	912.43	3.89	-3.48	-2.36	896.01	11.00	-5.22	-4.12
	100	1102.64	37.86	1034.77	1.60	1038.42	7.16	-5.82	0.35	1014.65	20.51	-7.98	-1.94
	175	1469.92	41.58	1453.16	2.74	1457.59	21.84	-0.84	0.30	1408.44	107.60	-4.18	-3.08
	250	1635.12	196.27	1709.35	3.78	1762.70	44.51	7.80	3.12	1701.57	314.41	4.06	-0.46
	Average		41.46		1.43		11.36	-2.25	-0.78		65.67	-4.08	-2.61

Table 10: (TSPD Set A_L , limited) Results of HGA-TAC and HGA-TAC⁺ for Agatz et al. (2018)’s instances with limited flying ranges, where r is a parameter in the dataset that controls the maximum flying range. Times are in seconds.

N	r	TSP-ep-all		DPS/25		HGA-TAC		Gap over (%)		HGA-TAC ⁺		Gap over (%)	
		Obj	Time	Obj	Time	Avg.	Time	TSP-ep-all	DPS/25	Avg.	Time	TSP-ep-all	DPS/25
10	20	303.74	0.01	303.74	0.01	303.74	0.27	0.00	0.00	303.74	0.79	0.00	0.00
	40	295.73	0.01	295.73	0.01	295.60	0.28	−0.04	−0.04	295.58	0.77	−0.05	−0.05
	60	277.12	0.01	277.12	0.01	276.09	0.24	−0.37	−0.37	275.90	0.73	−0.44	−0.44
	100	236.02	0.01	236.02	0.01	235.47	0.23	−0.23	−0.23	235.30	0.69	−0.31	−0.31
	150	219.41	0.01	219.41	0.01	219.35	0.23	−0.03	−0.03	219.13	0.68	−0.13	−0.13
	200	218.57	0.01	218.57	0.01	218.19	0.21	−0.17	−0.17	218.07	0.54	−0.23	−0.23
	Average		0.01		0.01		0.24	−0.14	−0.14		0.70	−0.19	−0.19
20	5	396.30	0.03	396.30	0.03	396.30	0.50	0.00	0.00	396.30	1.69	0.00	0.00
	10	396.08	0.03	396.08	0.03	396.08	0.54	0.00	0.00	396.08	1.71	0.00	0.00
	15	394.58	0.03	394.58	0.03	394.50	0.58	−0.02	−0.02	394.47	1.75	−0.03	−0.03
	20	387.57	0.04	387.57	0.04	387.02	0.59	−0.14	−0.14	386.76	1.72	−0.21	−0.21
	30	359.79	0.04	359.79	0.04	359.98	0.53	0.05	0.05	359.45	1.63	−0.10	−0.10
	40	344.60	0.05	344.60	0.05	343.70	0.45	−0.26	−0.26	342.69	1.35	−0.56	−0.56
	50	322.02	0.05	322.02	0.05	320.00	0.47	−0.63	−0.63	319.45	1.41	−0.80	−0.80
	Average		0.04		0.04		0.53	−0.17	−0.17		1.59	−0.28	−0.28
50	5	595.57	0.53	595.57	0.08	595.58	2.38	0.00	0.00	595.57	8.07	0.00	0.00
	10	587.29	0.95	587.49	0.11	587.36	2.01	0.01	−0.02	587.25	5.93	−0.01	−0.04
	15	561.82	1.32	564.59	0.13	562.97	1.72	0.20	−0.29	561.40	5.92	−0.08	−0.57
	20	514.65	1.63	516.89	0.15	519.11	1.54	0.87	0.43	516.54	5.34	0.37	−0.07
	30	451.17	2.55	459.20	0.20	456.73	1.55	1.23	−0.54	451.88	5.21	0.16	−1.59
	40	418.46	3.85	431.86	0.25	426.10	1.98	1.83	−1.33	420.90	6.32	0.58	−2.54
	50	414.27	6.22	427.90	0.32	421.46	2.03	1.74	−1.51	413.24	7.22	−0.25	−3.43
	Average		2.75		0.19		1.80	0.98	−0.54		5.99	0.13	−1.37
75	5	629.48	3.29	629.48	0.13	629.56	4.85	0.01	0.01	629.45	15.06	0.00	0.00
	10	603.19	6.96	604.30	0.17	604.32	2.47	0.19	0.00	603.39	8.36	0.03	−0.15
	15	553.38	12.81	557.19	0.24	559.43	2.44	1.09	0.40	556.27	9.02	0.52	−0.17
	20	508.73	18.20	515.90	0.30	520.68	2.44	2.35	0.93	513.74	10.07	0.99	−0.42
	30	449.88	26.65	459.52	0.37	459.09	3.19	2.05	−0.10	452.11	10.65	0.49	−1.61
	40	436.16	49.10	445.09	0.49	449.37	3.25	3.03	0.96	440.41	12.68	0.98	−1.05
	50	433.02	80.76	439.36	0.62	445.77	3.10	2.95	1.46	435.56	12.91	0.59	−0.87
	Average		28.25		0.33		3.11	1.67	0.52		11.25	0.51	−0.61
100	5	780.32	13.58	780.43	0.18	780.38	9.14	0.01	−0.01	780.34	30.27	0.00	−0.01
	10	728.87	34.05	731.13	0.23	730.57	3.51	0.23	−0.08	729.00	13.55	0.02	−0.29
	15	654.82	64.33	660.33	0.33	664.36	3.48	1.46	0.61	660.37	14.32	0.85	0.01
	30	555.81	130.23	567.71	0.57	572.83	4.86	3.06	0.90	563.69	17.98	1.42	−0.71
	50	547.41	497.45	559.12	0.90	572.26	4.37	4.54	2.35	557.19	21.93	1.79	−0.34
	Average		147.93		0.44		5.07	1.86	0.76		19.61	0.81	−0.27

Table 11: (TSPD Set B) TSPD results on the datasets of Bogyrbayeva et al. (2023). Average cost and time values are reported on 100 problem instances for each size N . Times are in seconds, and Time* is as reported in Bogyrbayeva et al. (2023). Gap values are measured, in %, over the Obj values of TSP-ep-all, and the Avg. values are used for HGA-TAC and HGA-TAC⁺.

Dataset	N	TSP-ep-all		DPS/25			HM (4800)			HGA-TAC				HGA-TAC ⁺			
		Obj	Time	Obj	Time	Gap	Obj	Time*	Gap	Best	Avg.	Time	Gap	Best	Avg.	Time	Gap
Random	20	281.85	0.10	281.85	0.01	0.00	281.53	0.40	-0.11	278.25	280.42	0.36	-0.51	277.82	279.54	1.19	-0.82
	50	397.63	21.99	404.88	0.54	1.82	395.65	1.72	-0.50	394.64	402.52	1.36	1.23	389.12	396.11	4.69	-0.38
	100	535.20	2566.28	548.08	1.14	2.41	544.55	4.09	1.75	541.71	551.38	4.68	3.02	530.57	538.95	18.59	0.70
	Average	404.89	862.79	411.60	0.56	1.41	407.24	2.07	0.38	404.87	411.44	2.13	1.25	399.17	404.87	8.16	-0.17
Amsterdam	10	2.02	0.02	2.02	0.02	0.00	2.04	0.32	0.99	2.00	2.01	0.17	-0.50	2.00	2.00	0.57	-0.99
	20	2.36	0.09	2.36	0.09	0.00	2.38	0.52	0.85	2.32	2.34	0.36	-0.84	2.32	2.33	1.35	-1.27
	50	3.26	21.92	3.37	0.56	2.58	3.31	1.41	1.53	3.27	3.35	1.55	2.76	3.23	3.31	4.94	1.53
	Average	2.55	7.34	2.58	0.22	1.12	2.58	0.75	1.12	2.53	2.57	0.69	0.47	2.52	2.55	2.29	-0.24

Table 12: (FSTSP Set M) Results for FSTSP instances from Murray and Chu (2015). MC and HGA20 represent the results reported by Murray and Chu (2015) and Ha et al. (2020), respectively. Times are in seconds. Gap values are measured, in %, between the Avg. values of HGA-TAC and HGA-TAC⁺ and the Avg. values of HGA20.

Instance	ϵ	MC	HGA20		HGA-TAC				HGA-TAC ⁺			
			Best	Avg.	Best	Avg.	Time	Gap	Best	Avg.	Time	Gap
437v1	20	56.468	56.468	56.468	56.393	56.393	0.38	−0.13%	56.393	56.393	1.16	−0.13%
437v1	40	50.573	50.573	50.573	50.573	50.573	0.39	0.00%	50.573	50.573	1.18	0.00%
437v2	20	53.207	53.207	53.207	53.207	53.207	0.35	0.00%	53.207	53.207	1.11	0.00%
437v2	40	47.311	47.311	47.311	47.311	47.311	0.37	0.00%	47.311	47.311	1.13	0.00%
437v3	20	53.687	53.687	53.687	54.664	54.664	0.33	1.82%	54.664	54.664	1.11	1.82%
437v3	40	53.687	53.687	53.687	53.687	53.687	0.39	0.00%	53.687	53.687	1.16	0.00%
437v4	20	67.464	67.464	67.464	67.464	67.464	0.34	0.00%	67.464	67.464	1.10	0.00%
437v4	40	66.487	66.487	66.487	66.487	66.487	0.39	0.00%	66.487	66.487	1.17	0.00%
437v5	20	50.551	50.551	50.551	50.779	51.234	0.48	1.35%	50.030	51.048	1.38	0.98%
437v5	40	45.835	44.835	44.835	44.835	44.835	0.46	0.00%	44.835	44.835	1.14	0.00%
437v6	20	45.176	47.311	47.311	47.604	47.604	0.38	0.62%	47.604	47.604	1.12	0.62%
437v6	40	45.863	43.602	43.602	43.602	43.632	0.40	0.07%	43.602	43.627	1.34	0.06%
437v7	20	49.581	49.581	49.581	48.581	48.581	0.43	−2.02%	48.581	48.581	1.21	−2.02%
437v7	40	46.621	46.621	46.621	46.621	46.621	0.41	0.00%	46.621	46.621	1.15	0.00%
437v8	20	62.381	62.381	62.381	61.381	61.381	0.42	−1.60%	61.381	61.381	1.24	−1.60%
437v8	40	59.776	59.416	59.416	59.416	59.416	0.40	0.00%	59.416	59.416	1.17	0.00%
437v9	20	45.985	42.416	42.416	42.997	43.249	0.65	1.96%	42.712	42.851	1.36	1.03%
437v9	40	42.416	42.416	42.416	41.585	41.668	0.44	−1.76%	41.585	41.585	1.21	−1.96%
437v10	20	42.416	41.729	41.729	41.729	41.729	0.39	0.00%	41.729	41.729	1.07	0.00%
437v10	40	41.729	41.729	41.729	41.416	41.416	0.38	−0.75%	41.416	41.416	1.09	−0.75%
437v11	20	42.896	42.896	42.896	41.896	41.896	0.47	−2.33%	41.896	41.896	1.27	−2.33%
437v11	40	42.896	42.896	42.896	42.896	42.896	0.39	0.00%	42.896	42.896	1.14	0.00%
437v12	20	56.696	56.273	56.273	54.992	54.992	0.44	−2.28%	54.992	54.992	1.21	−2.28%
437v12	40	55.696	55.696	55.696	55.425	55.560	0.47	−0.24%	55.425	55.533	1.34	−0.29%
440v1	20	49.430	49.430	49.430	48.430	48.430	0.38	−2.02%	48.430	48.430	1.10	−2.02%
440v1	40	46.886	46.886	46.886	46.886	46.886	0.40	0.00%	46.886	46.886	1.14	0.00%
440v2	20	50.708	50.708	50.708	50.708	50.708	0.38	0.00%	50.708	50.708	1.15	0.00%
440v2	40	46.423	46.423	46.423	46.423	46.423	0.41	0.00%	46.423	46.423	1.16	0.00%
440v3	20	56.102	56.102	56.102	56.102	56.102	0.38	0.00%	56.102	56.102	1.14	0.00%
440v3	40	53.933	53.933	53.933	53.933	53.933	0.43	0.00%	53.933	53.933	1.20	0.00%
440v4	20	69.902	69.902	69.902	68.902	68.902	0.38	−1.43%	68.902	68.902	1.14	−1.43%
440v4	40	68.397	68.397	68.397	67.397	67.459	0.44	−1.37%	67.397	67.397	1.30	−1.46%
440v5	20	43.533	43.533	43.533	44.456	44.456	0.37	2.12%	43.533	43.533	1.06	0.00%
440v5	40	43.533	43.533	43.533	43.533	43.533	0.38	0.00%	43.533	43.533	1.07	0.00%
440v6	20	44.076	43.949	43.949	43.949	43.949	0.34	0.00%	43.949	43.949	1.12	0.00%
440v6	40	44.076	43.810	43.853	43.810	43.810	0.35	−0.10%	43.810	43.810	1.04	−0.10%
440v7	20	49.996	49.422	49.422	48.422	48.422	0.36	−2.02%	48.422	48.422	1.08	−2.02%
440v7	40	49.204	49.204	49.204	48.470	48.470	0.37	−1.49%	48.470	48.470	1.11	−1.49%
440v8	20	62.796	62.576	62.576	61.222	61.222	0.35	−2.16%	61.222	61.222	1.07	−2.16%
440v8	40	62.270	62.004	62.004	61.270	61.270	0.35	−1.18%	61.270	61.270	1.06	−1.18%
440v9	20	42.799	42.533	42.533	42.267	42.426	0.32	−0.25%	42.267	42.453	0.93	−0.19%
440v9	40	42.799	42.533	42.533	42.267	42.400	0.31	−0.31%	42.267	42.347	1.06	−0.44%
440v10	20	43.076	43.076	43.076	42.342	42.549	0.41	−1.22%	42.342	42.618	1.29	−1.06%
440v10	40	43.076	43.076	43.076	42.342	42.691	0.39	−0.89%	42.342	42.549	1.13	−1.22%
440v11	20	49.204	49.204	49.204	48.030	48.187	0.30	−2.07%	48.030	48.169	1.19	−2.10%
440v11	40	49.204	49.204	49.204	48.204	48.204	0.29	−2.03%	48.204	48.204	0.95	−2.03%
440v12	20	62.004	62.004	62.004	60.610	60.715	0.46	−2.08%	60.610	60.632	1.54	−2.21%
440v12	40	62.004	62.004	62.004	61.004	61.004	0.28	−1.61%	61.004	61.004	0.94	−1.61%
443v1	20	69.586	69.586	69.586	69.586	69.586	0.37	0.00%	69.586	69.586	1.13	0.00%
443v1	40	55.493	55.493	55.493	56.676	56.877	0.40	2.49%	55.493	55.576	1.15	0.15%

Table 12: (Continued)

Instance	ϵ	MC	HGA20		HGA-TAC				HGA-TAC ⁺			
			Best	Avg.	Best	Avg.	Time	Gap	Best	Avg.	Time	Gap
443v2	20	72.146	72.146	72.146	72.146	72.146	0.37	0.00%	72.146	72.146	1.12	0.00%
443v2	40	58.053	58.053	58.053	58.053	58.053	0.39	0.00%	58.053	58.053	1.13	0.00%
443v3	20	77.344	77.344	77.344	77.344	77.344	0.37	0.00%	77.344	77.344	1.12	0.00%
443v3	40	69.175	68.431	68.431	68.431	68.431	0.59	0.00%	68.431	68.431	1.56	0.00%
443v4	20	90.144	90.144	90.144	90.144	90.144	0.38	0.00%	90.144	90.144	1.10	0.00%
443v4	40	82.700	82.700	82.700	82.700	82.700	0.42	0.00%	82.700	82.700	1.15	0.00%
443v5	20	55.493	54.973	55.077	54.973	55.435	0.40	0.65%	54.973	55.146	1.13	0.13%
443v5	40	53.447	51.929	51.929	51.422	51.523	0.49	−0.78%	51.422	51.625	1.81	−0.59%
443v6	20	58.053	55.209	55.209	55.209	56.174	0.39	1.75%	55.209	55.673	1.10	0.84%
443v6	40	52.329	52.329	52.329	52.289	52.289	0.40	−0.08%	52.289	52.289	1.20	−0.08%
443v7	20	64.409	65.523	65.523	64.523	64.523	0.39	−1.53%	64.523	64.523	1.08	−1.53%
443v7	40	60.743	60.743	60.743	60.743	61.086	0.48	0.56%	60.743	61.164	1.42	0.69%
443v8	20	77.209	78.323	78.323	78.323	81.561	0.40	4.13%	78.323	79.183	1.12	1.10%
443v8	40	73.967	72.967	72.967	72.481	72.481	0.44	−0.67%	72.481	72.481	1.21	−0.67%
443v9	20	49.049	45.931	45.931	45.931	45.931	0.37	0.00%	45.931	45.931	1.07	0.00%
443v9	40	47.250	45.931	45.931	45.931	45.931	0.42	0.00%	45.931	45.931	1.10	0.00%
443v10	20	47.935	46.935	46.935	46.935	47.735	0.48	1.70%	46.935	46.935	1.27	0.00%
443v10	40	47.935	46.935	46.935	46.935	47.735	0.42	1.70%	46.935	46.935	1.16	0.00%
443v11	20	57.382	56.395	56.395	55.395	55.395	0.37	−1.77%	55.395	55.395	1.03	−1.77%
443v11	40	56.395	56.395	56.395	56.395	56.395	0.36	0.00%	56.395	56.395	1.00	0.00%
443v12	20	69.195	69.195	69.195	68.195	68.195	0.45	−1.45%	68.195	68.195	1.08	−1.45%
443v12	40	69.195	69.195	69.195	68.195	68.195	0.36	−1.45%	68.195	68.195	1.00	−1.45%
Average		55.215	54.937	54.939	54.659	54.785	0.40	−0.28%	54.616	54.677	1.16	−0.48%

Table 13: (FSTSP Set H) Results for FSTSP instances from Ha et al. (2018). Times are in seconds, and Time* represents the time reported in Ha et al. (2018). Gap is measured between the Avg. values of HGA-TAC and HGA-TAC⁺ and the Avg. values of HGA20.

Instance	HGA20			HGA-TAC				HGA-TAC ⁺			
	Best	Avg.	Time*	Best	Avg.	Gap	Time	Best	Avg.	Gap	Time
B1	115.65	116.43	45.60	116.92	117.23	0.69	2.73	115.11	115.89	-0.46	12.26
B2	118.39	118.39	19.80	113.93	114.17	-3.56	1.69	113.50	113.82	-3.86	9.06
B3	116.21	116.39	34.20	114.09	114.75	-1.41	2.59	112.25	113.52	-2.46	10.57
B4	118.71	119.26	28.20	119.85	121.77	2.11	2.05	119.19	120.88	1.35	10.38
B5	115.78	115.91	34.80	113.77	114.38	-1.32	1.84	112.77	114.44	-1.27	6.02
B6	114.31	115.46	52.80	114.04	115.25	-0.18	2.87	112.11	112.69	-2.40	12.07
B7	115.52	115.63	37.20	115.53	117.84	1.91	2.67	113.63	115.02	-0.52	12.56
B8	117.90	118.04	46.80	113.25	114.13	-3.32	2.41	113.25	113.70	-3.68	10.00
B9	117.64	117.72	23.40	116.23	117.14	-0.49	1.87	116.23	116.90	-0.69	7.89
B10	117.38	117.70	36.00	114.28	115.31	-2.03	2.77	114.28	115.04	-2.26	8.55
C1	215.07	215.37	36.00	214.91	216.34	0.45	2.12	211.80	212.38	-1.39	11.43
C2	209.23	210.11	31.80	202.41	202.82	-3.47	1.28	202.41	202.90	-3.43	4.03
C3	212.02	212.22	22.80	204.79	204.97	-3.42	1.29	204.79	204.97	-3.42	3.92
C4	212.08	213.27	36.00	215.25	218.72	2.55	1.75	212.17	215.12	0.87	9.43
C5	223.06	224.57	28.80	225.54	225.54	0.43	1.36	225.54	225.54	0.43	4.14
C6	234.01	235.56	18.60	233.57	233.57	-0.84	1.29	233.57	233.57	-0.84	4.10
C7	222.27	223.40	30.60	218.98	220.10	-1.48	2.27	219.00	219.49	-1.75	8.14
C8	234.26	237.53	27.60	233.44	234.68	-1.20	2.17	233.24	234.18	-1.41	8.22
C9	226.01	227.43	40.80	222.60	224.43	-1.32	1.15	222.60	224.73	-1.19	3.59
C10	226.17	226.17	28.80	222.99	223.88	-1.01	1.48	222.63	223.62	-1.13	6.50
D1	306.39	307.09	36.60	312.78	314.32	2.35	2.14	312.78	313.40	2.05	8.10
D2	313.93	315.64	34.20	306.78	308.79	-2.17	1.80	305.80	307.70	-2.52	5.84
D3	295.86	297.54	36.00	289.49	290.96	-2.21	3.17	286.82	288.30	-3.11	10.01
D4	323.72	324.60	33.60	320.80	321.96	-0.81	2.42	319.25	320.94	-1.13	7.88
D5	321.46	321.83	24.00	315.75	316.46	-1.67	2.27	313.82	314.08	-2.41	8.47
D6	313.21	313.65	29.40	307.81	308.06	-1.78	1.98	307.81	307.87	-1.84	6.34
D7	316.65	317.83	19.20	312.23	315.81	-0.64	2.40	309.42	314.25	-1.13	7.99
D8	293.76	296.51	34.80	291.31	294.37	-0.72	2.53	288.53	294.13	-0.80	6.14
D9	317.85	318.31	24.60	326.99	327.62	2.92	1.11	326.99	327.46	2.87	3.29
D10	305.51	305.54	24.60	298.20	300.20	-1.75	2.23	297.58	298.89	-2.18	7.03
E1	187.67	188.32	216.00	178.77	181.24	-3.76	8.63	177.03	178.10	-5.42	37.01
E2	187.21	188.01	336.00	182.60	183.51	-2.39	6.88	180.11	181.35	-3.54	27.21
E3	188.09	188.89	274.80	179.24	180.28	-4.56	7.40	177.22	178.42	-5.54	36.17
E4	186.23	186.99	281.40	182.80	185.38	-0.86	7.69	177.92	179.75	-3.87	51.61
E5	187.71	188.26	243.60	181.85	183.62	-2.47	7.07	179.50	182.04	-3.30	32.81
E6	189.16	189.44	290.40	182.25	183.46	-3.16	10.83	179.65	181.05	-4.43	45.30
E7	190.39	190.89	230.40	184.40	185.52	-2.81	10.75	181.05	182.41	-4.44	54.15
E8	189.02	189.54	253.20	182.10	182.84	-3.53	9.33	179.97	180.72	-4.65	41.37
E9	189.76	189.94	240.00	181.53	183.61	-3.33	8.69	179.20	180.70	-4.87	51.66
E10	189.45	189.91	204.00	184.79	184.84	-2.67	5.04	184.84	184.84	-2.67	17.90
F1	322.94	326.10	343.80	326.89	334.71	2.64	5.64	322.88	329.92	1.17	26.79
F2	308.74	310.89	314.40	310.48	316.07	1.66	4.16	305.40	309.56	-0.43	28.95
F3	309.67	313.55	336.60	322.41	323.23	3.09	2.37	322.41	322.90	2.98	7.81
F4	311.37	314.96	363.60	320.15	320.25	1.68	2.47	320.15	320.25	1.68	7.83
F5	314.82	317.83	394.20	322.93	324.89	2.22	2.52	321.33	324.76	2.18	9.31
F6	294.38	297.47	282.00	293.17	296.78	-0.23	7.92	288.86	292.16	-1.79	39.54
F7	311.41	316.15	295.20	307.14	308.15	-2.53	5.18	304.08	306.05	-3.19	22.09
F8	323.74	326.40	312.60	325.76	327.16	0.23	2.23	325.76	329.98	1.10	7.21
F9	315.56	318.47	279.60	327.85	328.11	3.03	2.22	327.85	327.98	2.99	7.19
F10	312.70	315.13	236.40	318.68	319.14	1.27	2.34	318.68	319.14	1.27	7.53
G1	417.92	425.19	267.00	412.54	414.79	-2.45	6.75	409.57	411.53	-3.21	31.62

Table 13: (Continued)

Instance	HGA20			HGA-TAC				HGA-TAC ⁺			
	Best	Avg.	Time*	Best	Avg.	Gap	Time	Best	Avg.	Gap	Time
G2	389.64	390.14	144.00	397.37	401.86	3.00	5.35	388.18	401.98	3.03	16.31
G3	411.47	415.14	294.00	423.77	426.58	2.75	6.20	421.24	422.68	1.82	28.78
G4	433.09	435.56	280.20	430.63	431.62	−0.90	2.32	430.63	431.43	−0.95	7.33
G5	421.05	422.49	268.80	421.60	422.01	−0.11	2.21	416.34	419.82	−0.63	15.96
G6	415.46	420.84	330.60	426.26	433.17	2.93	3.53	425.39	430.77	2.36	14.80
G7	409.31	412.14	312.60	403.57	403.61	−2.07	2.13	403.57	403.66	−2.06	6.85
G8	406.51	407.89	304.80	423.31	427.04	4.70	6.74	413.32	421.51	3.34	28.44
G9	428.16	435.75	354.60	440.10	444.52	2.01	4.97	438.46	441.23	1.26	26.69
G10	426.82	430.94	324.00	435.84	438.78	1.82	2.32	435.84	438.78	1.82	7.32
Average	260.99	262.64	159.44	260.66	262.37	−0.47	3.73	258.92	260.85	−1.13	16.29